UAV Photogrammetry in Stockpile Management: From Data Acquisition to Dynamic Visualization

By

Utsav Dahal

Thesis
Submitted to Flinders University
for the degree of

Masters in Geospatial Information Science

College of Science and Engineering
26 August 2024

TABLE OF CONTENTS

ABSTRACT

This study aims to tackle the inefficiencies of volume computation, monitoring and data visualization in conventional stockpile management practices with the use of UAV photogrammetry. Conventional methods employ labour-intensive, tedious and potentially dangerous processes prone to errors and delays. The main goals of this study are to establish a robust methodology for stockpile volume computation, development of a comprehensive stockpile database and the enhancement of existing methods of reporting and visualization of stockpile data.

The study consisted of monthly surveys performed at Whyalla Iron Making, Pellet Plant and Steel Makings sites throughout the year 2023. Using UAVs equipped with high-resolution cameras and aided by GNSS technology, precisely geolocated aerial images were utilized for photogrammetric 3D reconstruction of the aforementioned sites. Outputs such as densified point clouds, DSMs and orthophotos facilitated precise volume estimation and broad spatial and temporal analyses significantly reducing the time and labour required compared to conventional techniques.

The integration of ArcGIS desktop and online platforms helped create an interactive web platform (accessible here) for dynamic visualization and effective monitoring of stockpiles. This platform enables stakeholders to explore data with user friendly interface facilitating data exploration, improved decision-making and enhanced communication. With interactive features such as dynamic timeline, charts, pop-ups and real-time data access, this platform offers a complete solution for modern stockpile management.

The findings of this study demonstrate the effectiveness of UAV photogrammetry in stockpile management with high precision, reduced costs and improved safety leading to notable increases in efficiency and offering benefits in operational planning and inventory management. Overall, this study presents the potential of advanced geospatial technologies in revolutionizing stockpile management. This also provides a framework for the use of UAV photogrammetry for future applications in a variety of industries.

DECLARATION

I certify that this thesis does not incorporate without acknowledgment any material previously submitted for a degree or diploma in any university; and that to the best of my knowledge and belief it does not contain any material previously published or written by another person except where due reference is made in the text.

Signed: 

Date: 26/08/2024

ACKNOWLEDGEMENTS

This study has been possible due to the help and guidance of many individuals. I would like to take this opportunity to acknowledge the contributions of all these individuals without which the study would not be complete.

Firstly, I would like to express my deepest gratitude to the Department of Geospatial Sciences at Flinders University for allowing me to pursue this study. Alongside, I would also like to thank the Remote Sensing and Geodesy (RS&G) team at Alexander and Symonds Surveying Consultancy for providing the means and the opportunity for this study to be conducted.

I am incredibly grateful to my supervisor, Tessa Lane for all the support and guidance I have received throughout this project. This study would not have been possible without her support. Thank you for your patience while I wavered around different ideas until I could finally settle down on one. Similarly, I would also like to thank all the other academic staff who have helped me during my journey laying strong foundations to conduct this study.

Special thanks to my wife, Asmita for her support as a colleague and a partner. Without you pushing me to my limits, I'd definitely be stuck at many hurdles.

I'd like to thank all my colleagues in the RS&G team and my academic peers at Flinders MGIS program for their help and support at various stages of this study.

I'd also like to thank all my family and friends for their belief and support. Finally, thanks to all the other individuals who contributed to this study in a direct or an indirect manner whose name I've failed to mention here.

LIST OF FIGURES

LIST OF TABLES

LIST OF ABBREVIATIONS

3DR	Cyclone 3D Reshaper
A&S	Alexander and Symonds Surveying Consultancy
AHD	Australian Height Datum
AT	Aerial Triangulation
CAD	Computer Aided Design
CSV	Comma Separated Values
CV	Coefficient of Variation
CORS	Continuously Operating Reference Stations
DEM	Digital Elevation Model
DTM	Digital Terrain Model
DSM	Digital Surface Model
DXF	Drawing Interchange Format
EDM	Electronic Distance Measurement
GCP	Ground Control Point
GDA94	Geocentric Datum of Australia 1994
GDA2020	Geocentric Datum of Australia 2020
GIS	Geographic Information System
GNSS	Global Navigation Satellite System
GPS	Global Positioning System
GSV	Google Street View
IMU	Inertial Measurement Unit
IOP	Interior Orientation Parameters
JS	Javascript
JSON	Javascript Object Notation
LiDAR	Light Detection and Ranging
PPK	Post-Processed Kinematics
QGIS	Quantum Geographic Information System
RPAS	Remotely Piloted Aircraft Systems
RTK	Real-Time Kinematics
SBAS	Satellite-Based Augmentation System

SMART	Stockpile Monitoring and Reporting Technology
TIN	Triangulated Irregular Network
TLS	Terrestrial Laser Scanning
TS	Total Station
SfM	Structure from Motion
sUAS	Small Unmanned Aerial System
UAV	Unmanned Aerial Vehicle

1 INTRODUCTION

1.1 Background

The diversity of materials for use in a range of industries: from the enormous piles of sand, cement and gravel that underpin the growth of our infrastructure to the glistening heaps of precious metals that are refined into jewellery and the vital elements procured for high-tech uses such as silicon for computer chips and cell phones, lithium for batteries and rare earth metals all start their journey being stockpiled. Effective management of these stockpiles is crucial for industry-wide economic viability as well as operational success. However, proper measurement and monitoring of these stockpiles can be very challenging. The agencies in charge of stockpile management have had to resort to labour-intensive, time consuming and dangerous techniques to measure and monitor their stocks. Better management leads to improved technical analysis, budgeting, price prediction, safety, inventory management, and regulatory compliance providing significant gains in operations.

Stockpile management is a form of inventory management applicable in a multitude of industries. The principle is to optimize stock volume while minimizing costs. Effective inventory management is achieved when shortages are avoided while minimizing excess inventory costs (Tersine and Toelle, 1984). Gregory et al. (2021) state that automated inventory tracking using advanced technologies such as computer vision and robotic imaging systems can replace costly, error-prone human input and provide an efficient and cost-effective solution. In the world of stockpile management, Unmanned Aerial Vehicles (UAVs) provide this solution.

1.1.1 Technological Advancements in Stockpile Management

The methods to achieve the needs of stockpile management have evolved over the years. With the technological advancements of the 21st century, innovative solutions have emerged revolutionizing the stockpile management practices. Leading the way in this transition are sophisticated photogrammetry methods and UAVs. Regardless of the material, UAV photogrammetry has demonstrated remarkable potential for obtaining precise and effective stockpile volume estimates. Ai et al. (2015) and Adjidjonu and Burgett (2019) have shown the efficacy of UAV technology in improving efficiency and safety by providing accurate measurements through detailed 3D models with minimal human intervention.

1.1.2 Benefits of UAV Photogrammetry

The versatility of UAVs enables operation in difficult and dangerous environments. Alsayed et al. (2021) and Manish et al. (2022) showcased the application of UAV assisted inspections in confined spaces that present several safety risks for conventional methods whereby high-resolution data was gathered leading to precise volume estimations while ensuring the safety of the operators. Additionally, this approach does not have a negative impact on volume accuracy. In fact, Arango

and Morales (2015) and Raeva et al. (2016) found that UAV based surveying can outperform the conventional survey techniques. Their detailed study in accuracy comparisons with traditional survey methods promise a transformation from the existing methods of stockpile management across several industries such as forestry, agriculture, construction and manufacturing.

The most significant benefit of UAV photogrammetry is the reduction in computational time and costs. Traditional methods require a higher number of manpower and consume longer time to complete extending timelines. In contrast, surveys conducted with UAVs finish faster and with fewer workers needed on site. UAVs save labour costs and speed up data collection by eliminating the need for ground-based surveys, as noted by Ajayi and Ajulo (2021). In addition, UAV photogrammetry's great precision and detail can save expensive mistakes and rework, which can result in significant long-term savings.

1.1.3 Challenges in UAV Photogrammetry

The accuracy of volume estimates is dependent on the needs of the industry. The limitations of stand-alone photogrammetry in accurate volume estimations can be mitigated through the use of Ground Control Points (GCPs). The effects of GCP quantity and distribution on the precision of resultant photogrammetric models was investigated by Awasthi et al. (2019) highlighting the significance of strategic planning in UAV survey missions. Additionally, the integration of UAV with LiDAR technology has opened new possibilities for the capture of reliable and accurate volumetric data (Gaspari et al., 2022). The combination of these two approaches can provide solutions to various stockpile environments.

1.2 Evolution of Stockpile Volume Computation Methods

The methods of stockpile volume computation have evolved over time with technological advancements. The earliest volume computation methods relied on basic tools such as tape measures and chains and utilized simple mathematical formulas to estimate volume. The volume computation for irregularly shaped objects involved breaking the object down into multiple smaller and manageable sub-geometries and computing volumes of each sub-geometry. Several methods were developed over the years to simplify volume calculations of varying shapes (Twigg, 1995). Chambers (1989) devised a methodology for volume estimation of pit excavation using unequal intervals. Despite the simplicity of these methods, these approaches are susceptible to errors and inconsistencies, particularly for large irregular objects such as stockpiles. In addition, this approach also requires extensive manual labour (Alsayed and Nabawy, 2023; Son et al., 2020).

1.2.1 Truckload Counting: A Crude yet Common Approach

Several methods of stockpile volume computation have been developed over the years. Truckload counting is a popular method whereby a truckload of material is used as a reference measurement and the total volume is computed by counting the truckloads. In case of small stockpiles, a

bucketload is used as a benchmark for volume computation. This is the crudest form of volume estimation with high variability and low accuracy. Counting truckloads/bucketloads is not a practical solution for large stockpiles or dynamically changing stockpiles (Alsayed and Nabawy, 2023; Son et al., 2020).

1.2.2 Total Station (TS) Surveys: Precision at the Expense of Labour

During the 1980s and 1990s, TS became a critical technology in the construction industry. Initially introduced around 1975, TS combined electronic distance measurement (EDM) and angle measurement into a single device, allowing tacheometric computations to be done within the instrument and providing real-time 3D point co-ordinates. This significantly enhanced the efficiency and accuracy of several surveying tasks including volume computation. By the 1990s, robotic total stations revolutionized the industry by enabling a single operator to operate the equipment further reducing the need for manual labour (Lemmens, 2016; Brown et al., 2007).

Total station (TS) surveys of stockpile involve manual measurement of points on the stockpile. This requires a surveyor to climb on the stockpile with a target prism to obtain the co-ordinates of points in 3D space. After sufficient point co-ordinates have been recorded, the stockpile surface can be created in the form of a Triangulated Irregular Network (TIN) which is then used to estimate the volume of the stockpile. This method is precise but slow and requires physical interaction with materials which may involve health hazards (Alsayed and Nabawy, 2023; Son et al., 2020).

1.2.3 Global Navigation Satellite System (GNSS) Surveying: Balancing Efficiency and Accuracy

The introduction of GNSS systems in the 1990s provided surveyors further enhanced the volume computation methods. With increased availability of satellite data and GNSS receivers, the application of GNSS systems extended from general positioning and navigation to surveying and volume computation. By the early 2000s, GNSS became a staple in the surveying industry due to its capabilities of precision over large areas.

Compared to TS, GNSS surveying offers a slightly less precise way of getting the point co-ordinates in a more time efficient manner and requires less operator surveying skills. The accuracy can be improved using external data from Continuously Operating Reference Stations (CORS) or established local base stations. Real-Time Kinematics (RTK) that provides real-time correction to errors inherent in GNSS observations while Post-Processed Kinematics (PPK) generates correction values after the completion of the survey (Lau & Tai, 2023). PPK provides a higher accuracy than RTK corrections while adding processing time (Famiglietti et al., 2021). Like TS surveys, the major disadvantage to this method is that it too requires manual interaction with materials.

1.2.4 Terrestrial Laser Scanning (TLS): Automating Precision Measurement

TLS emerged as a tool for volume computation in the early 2000s driven by advancement in scanning and data processing technologies. By mid-2000s, TLS was being increasingly used for accurate volumetric measurements (Yao et al., 2017). Through the 2010s, this technology has evolved with consistent improvements in scanner range, resolution and processing software. Now, its usage has increased to include applications such as deformation monitoring, quality assessment and 3D model reconstruction. The ability of a TLS to deliver dense and accurate topographic data makes it an invaluable tool for precise volume computations (Wu et al., 2022; Yao et al., 2017). TLS has significantly aided the field of volume computation offering high precision and efficiency. TLS surveys utilize a laser scanner placed on a rotating platform automatically performs many measurements of stockpile surface to produce a point cloud. A point cloud is a collection of 3 dimensional points in space that represents the scanned object.

The problem of needing to climb up stockpiles to get the co-ordinates of relevant points is solved with the use of a TLS. After the scanner is placed at multiple positions surrounding a stockpile, the stockpile can be recreated without any manual interaction with the materials (Yao et al., 2017). This has been the method of choice due to the ease-of-use, high precision, and ability to capture surface details. However, a ground-based laser scanner cannot always manage to capture the full height of a stockpile. If the stockpile has a large base and height, the top plateau is obscured for laser-based measurements. Even with the use of a laser scanner, the survey team still needs to be on-site and close to the stockpile making the crew prone to all sorts of hazardous conditions.

1.2.5 UAVs Revolutionizing Stockpile Volume Estimation

The early 2010s marked a significant breakthrough with the adoption of UAVs equipped with high resolution cameras in a multitude of applications. With the help of photogrammetry software that process overlapping aerial images to create accurate 3D models, UAVs or Remotely Piloted Aircraft Systems (RPAS) started being used for volume computation. UAVs offer a low-cost robotic solution for difficult inventory management jobs by securely improving the accuracy of stockpile volume estimations in confined areas (Alsayed et al., 2021). Although the relationship between inventory management and profitability has been shown to be correlated, safe deployment of stockpile measurement and inspection tasks is still difficult and labour-intensive. This could be caused by a combination of factors such size, uneven shape, and health risks associated with the manufacturing of raw materials and finished goods (Alsayed et al., 2021).

With findings within 3% of Terrestrial Laser Scanning (TLS) measurements, small Unmanned Aerial System (sUAS) photogrammetry offers a precise substitute for traditional techniques in measuring stockpile height and volume (Mora et al., 2020). Accurately estimating the quantity of material to be stockpiled for construction projects can have a substantial impact on public safety, project deadlines, and costs. These stockpiles can now be estimated at a fraction of the cost and time of old methods

utilising low-cost aerial imaging and photogrammetry, thanks to the recent growth sUAS platforms (Mora et al., 2020). The author also stated that further improvements in accuracy can be made with improvements in data collection, processing, and modelling techniques. Manish et al (2022) reported a 1% relative error with reference to TLS measurements when deploying the Stockpile Monitoring and Reporting Technology (SMART) mapping platform for estimation of stockpile volume in challenging environmental conditions. For organisations and companies to keep an inventory of bulk commodities like aggregate, sand, lime, salt, and many other materials frequently used in industrial, highway, and agricultural applications, stockpile quantity monitoring is essential. Conventional methods, such as truckload counting, for volumetric evaluation of bulk material stockpiles are imprecise and prone to accumulated errors over an extended period. For performing high-fidelity geometric measurements, contemporary aerial, and terrestrial remote sensing systems with camera and/or Light Detection and Ranging (LiDAR) units have grown in popularity (Manish et al, 2022). Liu et al (2023) utilized SMART to estimate stockpile volume with LiDAR systems in dome facilities and reported point cloud alignments with a feature fitting error in the range of 0.03-0.08m range.

1.3 Advantages of UAV Photogrammetry

Stockpile volume estimation has traditionally relied on conventional techniques like truckload counting, Total Station (TS) surveys, and Global Navigation Satellite System (GNSS) surveying. These techniques, however, frequently entail a large amount of work, time, and possible safety hazards. Precise manual measurements are necessary for TS surveys, which can be time-consuming and labour-intensive. Even with increased automation, GNSS surveys still require a significant amount of physical labour and can be dangerous when surveyors must scale stockpiles to get precise coordinates. On the other hand, UAV photogrammetry drastically cuts down on the time and labour needed to acquire data. UAVs can take far less time than ground-based techniques to obtain high-resolution aerial photos. In contrast to a 5-hour survey duration using GNSS devices, Raeva et al. (2016) revealed that UAV-based data collecting took less than 30 minutes with a difference of 1.1% in volume. In open pit quarries, where monitoring constantly shifting stockpiles necessitates regular and thorough data gathering, this efficiency is especially helpful. In addition, countries also regulate the reporting accuracy of mining materials making it imperative for mining companies to improve their volume estimates.

Furthermore, by removing the necessity for surveyors to physically traverse dangerous stockpile terrain, UAV photogrammetry improves safety. With the processing of the high-resolution imagery obtained by UAVs, comprehensive 3D models may be created, offering accurate volumetric measurements without the hazards associated with conventional techniques. He et al. (2019), for example, discovered that UAV-based photogrammetry produced a slight variance of around ±2% in comparison to conventional human measurements. Likewise, Halim et al. (2023) demonstrated that

UAV photogrammetry produced data with an error rate of less than 3%, indicating a high level of efficiency and accuracy.

Additionally, it has been demonstrated that UAV-derived digital terrain models (DTMs) provide accuracy on par with airborne LiDAR, but at a reduced cost, particularly for small to medium-sized projects (Hugenholtz et al., 2015). Moreover, UAV techniques make it easier to create high-resolution 3D models, which are essential for accurate volumetric measurements (Tucci et al., 2019).

All things considered, UAV photogrammetry presents a strong substitute for conventional stockpile volume estimating techniques. The combined results of several studies highlight the benefits of using UAV technology to improve operational decision-making and streamline volumetric measurements.

By contrasting UAV photogrammetry with other precise measurement methods like Terrestrial Laser Scanning (TLS), the accuracy of UAV photogrammetry in stockpile volume estimate has been verified. According to studies (He et al., 2019; Mora et al., 2020), UAV photogrammetry may get accuracy within 3% of TLS measurements. These results are further supported by this study, which shows that volume estimates produced from UAVs are extremely dependable and compatible with accepted practices.

The geometric precision of the photogrammetric models is further improved by integrating Ground Control Points (GCPs) and using Real-Time Kinematic (RTK) or Post-Processed Kinematic (PPK) placement. GCPs guarantee exact spatial reference, while RTK/PPK methods offer perfect camera placement for taking pictures. These improvements are essential for minimising errors and distortions during the photogrammetric reconstruction procedure, which will produce precise volumetric measurements and accurate Digital Surface Models (DSMs) (Halim et al., 2023).

The operational efficiency and cost-effectiveness of UAV photogrammetry are among its most significant advantages. Traditional approaches come with large upfront expenditures and continuous operating expenses, particularly when they use cutting-edge technology like LiDAR. Although LiDAR systems—which estimate distance using laser pulses—offer unmatched precision, they are costly to buy and maintain. Additionally, the data processing for LiDAR is complicated and demands a significant amount of computational power and experience (Shaw et al., 2019; Gaspari et al., 2022).

On the other hand, UAV photogrammetry drastically lowers initial and ongoing expenses by using consumer-grade cameras and easily accessible software. UAVs can be swiftly and effectively deployed, enabling rapid data capture without requiring a lot of physical labour. Compared to LiDAR, photogrammetry's processing software is more user-friendly, enabling faster and more accessible data analysis (Chen et al., 2017; Mlambo et al., 2017). This affordability makes UAV photogrammetry is a desirable choice for regular stockpile monitoring duties. With volumetric evaluations, organisations may get great accuracy without incurring the expense burden of more sophisticated

technology. The method's overall efficiency and practicality are further enhanced by the decreased requirement for manual intervention, which also results in lower labour costs and reduced risks of injuries (Khanal et al., 2020).

To summarise, the selection of a stockpile volume computation technique is contingent upon a number of criteria, such as the need for accuracy, efficiency, and safety issues. Even though conventional techniques like total station surveys and truckload counting are precise, they can be dangerous for surveyors to use and are frequently labour-intensive. However, while more automation and efficiency are offered by cutting-edge technologies like TLS and GNSS surveying, in some situations manual involvement may still be necessary. When compared to conventional methods, UAV-based stockpile volume estimating techniques offer a number of advantages in terms of efficacy, precision, and affordability. It is anticipated that as technology and methods continue to progress, stockpile volume estimation will become increasingly accurate and reliable, improving inventory management procedures in a variety of industries. Organisations can improve operational efficiency and resource management in stockpile volume reporting by selecting the best strategy based on their unique needs by knowing the advantages and disadvantages of each method.

This study utilizes aerial photogrammetry for stockpile volume estimation. The following section describes the key photogrammetric concepts for the regeneration of a real-world object in a 3D model using aerial photogrammetry.

1.4 Volume Computation using Airborne Photogrammetry

Photogrammetry is the science of extraction of precise measurements (distances, angles, volumes, and spatial relationships) and 3D representations of objects and surfaces with the use of overlapping photos. Terrestrial photogrammetry deals with photos taken from the surface of the earth while airborne photogrammetry utilizes imagery taken from an aircraft or any other airborne platform. The advancement in the integration of Inertial Measurement Units (IMUs) and GNSS devices on UAVs in recent years has led to its extensive use in ground surface modelling. UAVs equipped with IMU/GPS units and high-resolution cameras are flown over areas of interest to generate overlapping aerial images with known positions in space and orientation of images (Colomina & Molina, 2014). The 3D co-ordinate accuracy can be further enhanced using GNSS techniques of PPK or RTK to get images with high positional accuracies (Jiménez-Jiménez et al., 2021). These images can then be processed in an image processing software to generate ground models in formats such as point clouds, Digital Terrain Models (DTMs), Digital Surface Models (DSMs), orthophotos, etc. In this study, point clouds are used to create 3-dimensional TIN meshes of stockpiles, which are then used to calculate volumes (Dai and Jiying, 2022). This allows for precise and efficient volume computation of stockpiles.

1.5 Reporting and Visualization

Alongside precise and efficient volume computation, accurate reporting and informative visualization are essential components of stockpile management. A comprehensive database of stockpile information plays a vital role in boosting operational efficiency and decision-making. Especially in cases of sites with large number of stockpiles, a database significantly enhances the organization and management of data providing convenient access to historical data. Multiple layers of data such as survey information, material properties and volumetric information can be organized in a structured format, facilitating storage and analysis. With the help of an integrated database, the management authority can ensure centralized data management while lowering the possibility of data loss or duplication (Elmasri & Navathe, 2011). Additionally, databases can utilize constraints and validation rules to maintain data integrity, guaranteeing the accuracy and dependability of stored data (Hoffer, Ramesh, & Topi, 2019). Furthermore, data access can be structured to meet the needs to several types of users ensuring effective data retrieval while concealing confidential data (Connolly & Begg, 2014).

The conversion of raw data to useful insights requires the use of effective reporting tools. With the help of these tools, reports can be tailored to meet the needs of different stakeholders. This study utilizes GIS platforms such as QGIS, ArcGIS Pro and ArcGIS Online for the generation of static and dynamic maps for data visualization. These tools allow detailed analysis of data, can display historical trends and comparative analysis providing a thorough overview of the stockpile dynamics. These tools also allow for automation in reporting enabling the generation of reports with minimal human intervention, standardizing procedures while ensuring timely updates. Similarly, these tools can also be used to customize templates to specific requirements, enhancing data relevancy and usefulness while simplifying complex information. The use of maps, graphs, charts and 3D models helps user comprehend complicated data patterns and relationships (Kirk, 2016). Additionally, the use of an online platform allows interactivity with data enabling in-depth analysis and discovery of insights through dynamic data exploration. Effective data visualization enhances communication with stakeholders providing relevant information and supporting decision making (Tufte, 2001).

1.6 Key Concepts in Photogrammetry

1.6.1 Collinearity Principle of Photogrammetry

The fundamental principle of photogrammetry is the collinearity concept. It involves determining how the picture, camera/sensor, and ground space relate to one another in order to translate the image coordinate system into the ground coordinate system, allowing for direct computation from the image (Linder, 2023). There is one distinct image point for every object point. On the other hand, there are an endless number of object points for every picture point. Consequently, reconstructing an item from a single photograph is not feasible. Each object must be seen in at least two photographs in order to complete this puzzle (Wolf et al, 2014). There are six basic elements of the Collinearity equation (Linder, 2023).

i. A Rotation matrix (M) that is formed using three rotation angles.
ii. Coordinates of the object point and centre of perspective in the object coordinate system.
iii. Coordinates of the image points and principal points in the image coordinate system.
iv. The scale factor (ratio of the focal length to the flying height in case of aerial cameras).

Figure 1 depicts the collinearity principle of photogrammetry whereby the image coordinate system corresponds to the ground coordinate system. It shows how an image point p can be accurately positioned on the ground with the help of the elements of the collinearity equation.

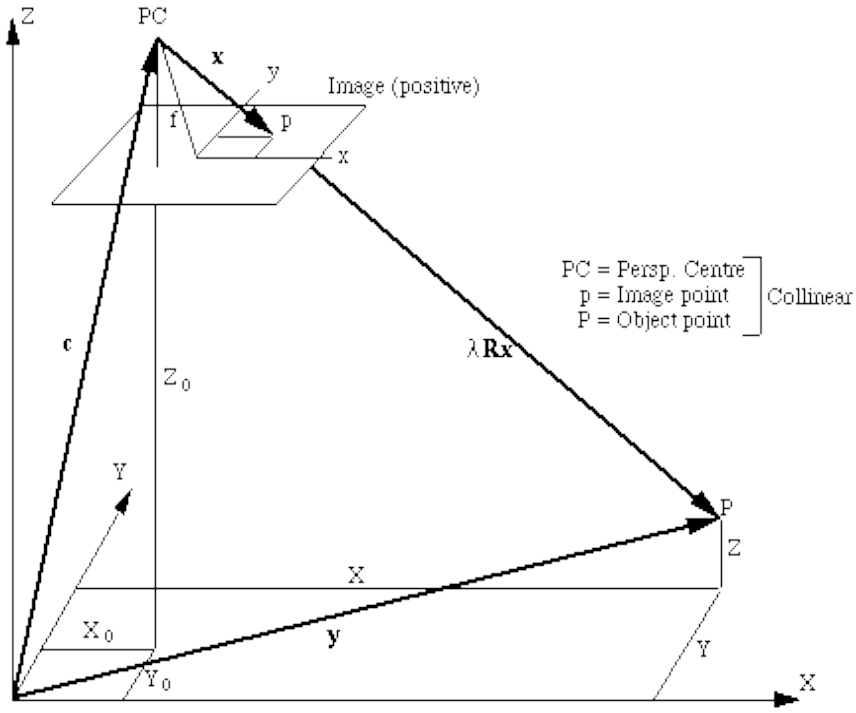

Figure 1: Collinearity principle of photogrammetry depicting the positioning of an image point on ground

1.6.2 Interior and Exterior Orientation

The process of aligning the geometry of the camera with the picture is known as interior orientation. It assists in converting the image pixel coordinate system to the image space coordinate system and describes the internal geometry of a camera or sensor as it was at the moment of image capture (Linder, 2023). In theory, a straight line is supposed to generate a spatial ray that is formed by the centre of perspective and the associated image point. Though, radiometric errors originate from the light beams' deviation from a straight line due to shifting refraction at the objective lens. Distortions can also happen in the direction perpendicular to the radial lines from the viewpoint centre referred to as tangential distortion. Correcting such distortions is necessary for a proper photogrammetric processing (Linder, 2023).

By defining what are known as IOP (Internal Orientation Parameters), one may determine the internal geometry of a camera. These are the lens distortion characteristics (tangential and radial), focal length, and principal point. The specifications of the internal orientation of digital cameras are

computed through a procedure called camera calibration (Roncella and Forlani, 2021). A crucial component of the photogrammetric process, the calibrated focal length has a big influence on the precision of the data and 3D models that are produced. When the lens is focused on a subject, the distance between the camera and the image sensor is referred to as the focal length in photogrammetry. According to Luhmann (2013), this distance is critical because it establishes the size of the photos that are taken, which is necessary to precisely recreate real-world dimensions in a 3D model. The calibrated focal length assures that the photogrammetry software can precisely stitch these photos together to build 3D models in the case of aerial photogrammetry. The accuracy of measurements obtained from these models, such as stockpile volumes or topographic characteristics, can be compromised by an incorrectly estimated focal length, which can result in mistakes in the scale and form of the reconstructed models (James et al., 2017). Furthermore, the usage of a calibrated focal length becomes even more crucial in industries where high accuracy is required, such as mining, construction, and surveying. Photogrammetry can obtain a better degree of precision and lower the margin of error in the final outputs by making sure the focal length is calibrated appropriately (Linder, 2023).

Exterior orientation establishes the relationship between image coordinate system and ground coordinate system (Linder, 2023). Determining the precise location and orientation of the camera during exposure is essential. Six parameters make up the external orientation of each image: three rotational angles (ω, φ, and κ) with respect to the object coordinate system's axes, and three spatial coordinates (X_0, Y_0, and Z_0) of the perspective centre in the object coordinate system. These variables help recreate an object in its true shape and location when paired with the values of the internal orientation. Fulfilling the Collinearity principle is the goal of exterior orientation (Linder, 2023).

1.6.3 Tie Points

Tie points are notable, consistent features that are identifiable in places where two or more images overlap and aid in computationally connecting (tying) the separate images to one another. They are the common spots where two or more photos overlap. They provide as a link between the photos in the block and are essential triangulation input. The distribution of tie points in a picture must be uniform throughout for orientation to be proper. The likelihood of improving the estimated picture parameters' correctness would increase with the number of evenly dispersed and precisely determined tie points (Linder, 2023).

1.6.4 Aerial Triangulation and Bundle block adjustment

The technique of creating a mathematical relationship among the images, the camera or sensor model, and the ground is known as Aerial Triangulation (AT) (Schenk, 1997). Here, the ground coordinates for each tie point produced by the image matching algorithm are calculated. The main benefit of AT is that it makes it easier to densify the network of ground control points based on the initial control points assessed, which helps to cut down on the time and money spent on field labour.

Bundle block adjustment involves specifying the mathematical 3D coordinates of those matched tie spots as well as adjusting AT (Roncella and Forlani, 2021). A block of imagery is processed using statistical methods to identify, distribute and remove error. It provides information on the exterior orientation parameters of each image and the ground co-ordinates of every tie point.

1.7 Research Problem

There is a notable gap in research about the application of Unmanned Aerial Vehicle (UAV) photogrammetry techniques to stockpile monitoring. Traditional methods are labour and time extensive and UAV photogrammetry has the potential to reduce survey operation time and decrease the amount of labour necessary. However, despite the advancements in UAV technology, its integration into routine stockpile management practices has not been optimized or standardized. In stockpile volume reporting, current standard operating procedures are frequently ineffective, especially when it comes to dissemination of information and communication. The use of spreadsheet-based procedures for monthly stockpile surveys has resulted in a considerable disparity in communication efficiency and data delivery, even with the introduction of UAV technology.

The use of an GIS technology can prove highly beneficial. Utilizing ArcGIS Web Experience platform as a dynamic interface for the analysis and visualisation of stockpile volume data is a key innovation in the suggested technique. This platform allows users to obtain detailed information on stockpile properties and allows real-time monitoring of volume changes over time. This unique technique provides a straightforward way of data exploration and analysis, while also improving communication efficiency by overcoming the limits of traditional spreadsheet-based reporting systems.

Given these factors, filling the identified gap requires a thorough examination of the effectiveness of UAV photogrammetry methods for stockpile monitoring, with an emphasis on enhancing data delivery and communication systems. By employing cutting-edge technology and optimising procedures, the suggested approach aims to fill in the gaps and provide a new way of thinking in the field of stockpile volume reporting.

1.8 Research Objectives

The research objectives are as follows:

i. Establishing a stockpile volume computation and monitoring methodology.
ii. Developing a comprehensive stockpile database.
iii. Enhancing stockpile volume reporting and visualization.
iv. Conducting temporal and spatial analyses of stockpile data.

1.9 Scope and Limitations

This study focuses on utilizing UAV based imagery for stockpile volume calculation. The main aim of this study is to explore the application of UAV photogrammetry in stockpile management from data acquisition to reporting and visualization. This study is grounded in literature review which leads into the design of the methodology. However, it does not involve the experimental manipulation of parameters to assess their individual impacts on accuracy or effectiveness of the photogrammetric process.

The scope of the study is intentionally focused on photogrammetry as a method for stockpile volume computation. Although alternative methodologies such as LiDAR exist, this study does not undertake a comparative analysis between Structure from Motion (SfM) photogrammetry and LiDAR based approaches. The rationale behind this is to maintain a clear and focused investigation within the domain of photogrammetry, without diverging into the technical differences and performance metrics between these two methods.

While this study provides valuable insights into the application of UAV photogrammetry for stockpile management, its scope is confined to a literature-based exploration of the topic. The exclusion of comparative analyses with LiDAR and the absence of parameter-specific experimentation represents the primary limitations of this research, which future studies could address to further enhance the understanding and application of UAV technologies in stockpile management.

2 STUDY AREA AND PERIOD

The study area is in Whyalla, South Australia (Figure 4). Alexander Symonds Surveying Consultants(A&S) conducts a monthly survey over stocks at Whyalla Iron Making, Steel Making and Pellet Plants for the GFG Alliance. These surveys are conducted using UAVs and 3D scanners. The schedule for the survey method for the company's various resources is detailed in Figure 3. This study was conducted from January 2023 to December 2023. A&S first begun conducting volumetric stockpile surveys using aerial imagery and TLS in December 2020 at Whyalla with gradual improvements in methodology and outputs generated. There are 12 UAV flights that cover the sites at 3 projects for image acquisition. Table 1 shows the mission names for the UAV flights and the sites they cover.

Table 1: UAV mission names and the corresponding sites that are surveyed in that mission

Mission Name	Surveyed Sites
Conveyor	Coal Conveyor, Limestone Pad, West Conveyor, South Scrapyard, Co Reserve
Quartz	Quartz Area
North Admin	North Admin
Wharf	Wharf
Scrapyard	Scrapyard
Skirun	Skirun, Coke Paddock, Slag, Coke Paddock South
Plant	Area 1, Filter Plant, Loadout, OHEF, Pellet Bins, OSPB
Highline	BF Highline
North Dimot	North Dimot
Steel Products Overflow Pad	Steel Products Overflow Pad
BIS Bins	BIS Bins
Refactory Warehouse	Refactory Warehouse, Second Bauxite Overflow Pad

The aerial surveys and the establishment of GCPs were conducted by A&S Remote Sensing and Geodesy (RS&G) team. The aerial images and GCP data thus acquired were utilized by the author in this research following the methodology presented in Chapter 3. Figure 2 presents the terrestrial imagery of stockpiles showing its scale.

Figure 2: Terrestrial images of large stockpiles depicting its size

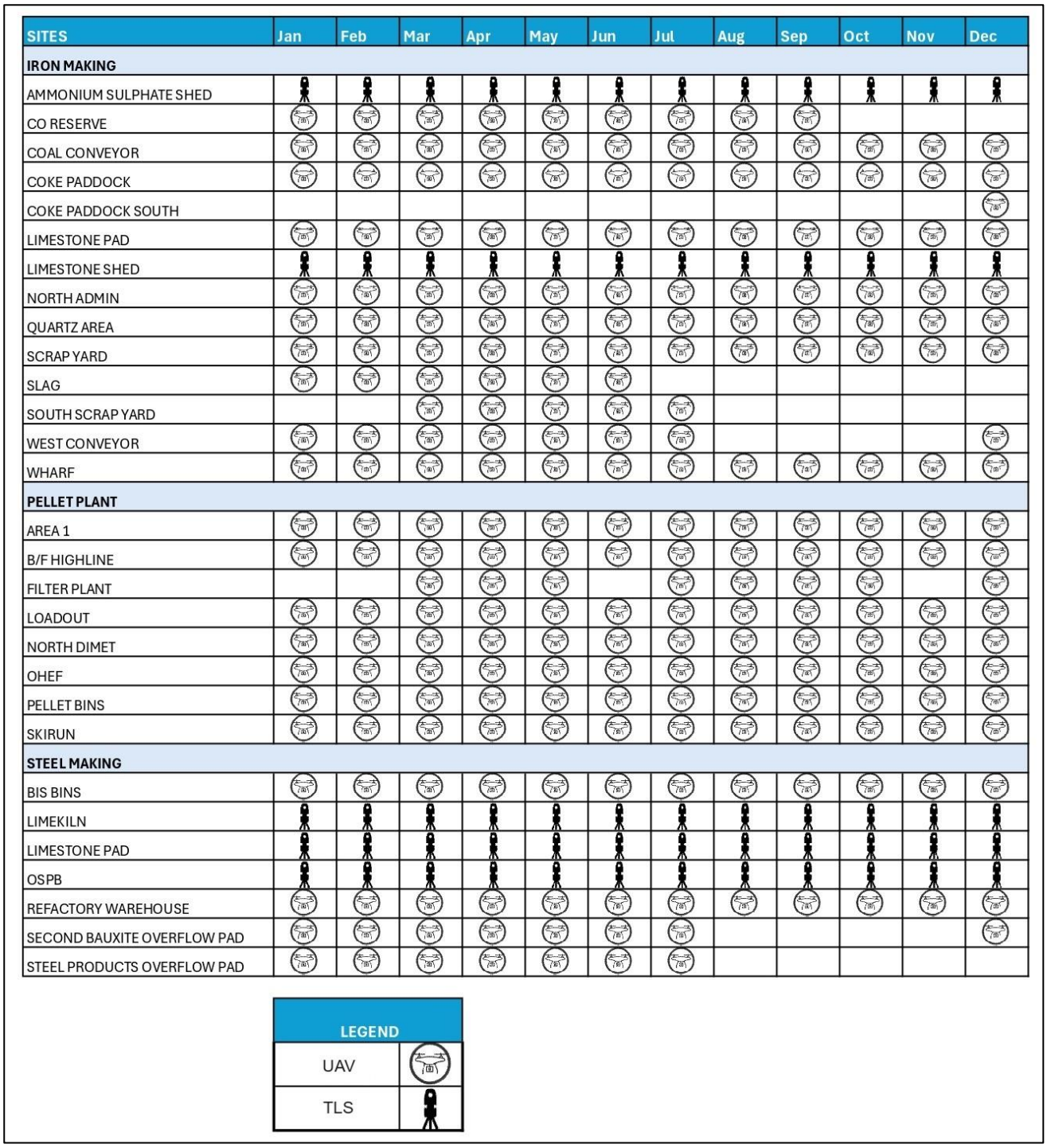

Figure 3: Type of Surveys conducted at selected sites in 2023.

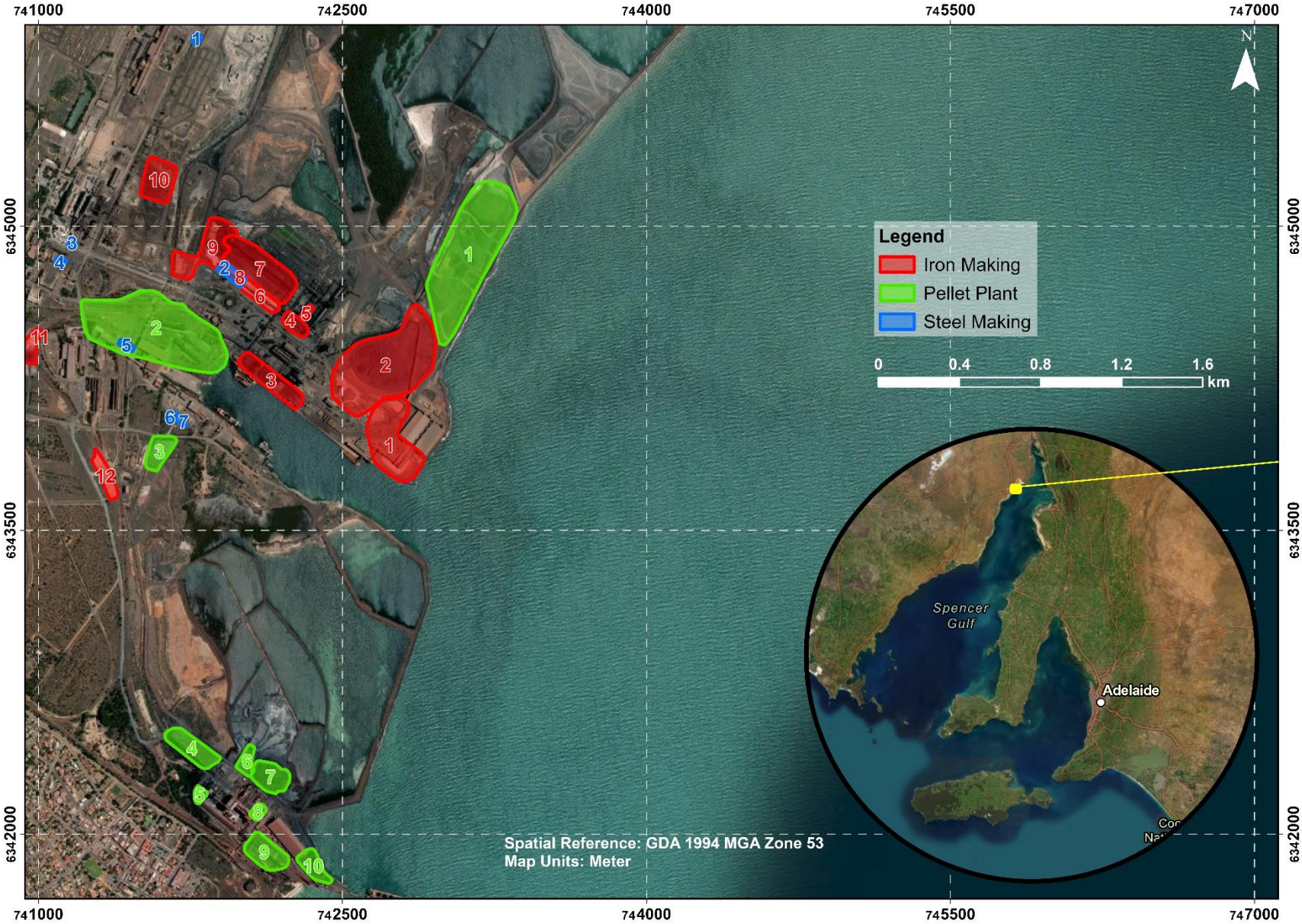

Figure 4: Map of the study area showing projects and sub-sites. The key to the label numbers of sub-sites is presented in Table 2

Table 2: Key to the study area labels where the colours of the label number text correspond to colour labels in Figure 4.

Iron Making		Pellet Plant		Steel Making	
Label No.	**Site Name**	**Label No.**	**Site Name**	**Label No.**	**Site Name**
1	Coke Paddock South	1	Skirun	1	Steel Products Overflow Pad
2	Coke Paddock	2	BF Highline	2	Limestone Pad
3	Wharf	3	North Dimot	3	Limekiln
4	Co Reserve	4	Area 2	4	BIS Bins
5	Sulphate Shed	5	Filter Plant	5	OSPB
6	Limestone Pad	6	Area 3	6	Refactory Warehouse
7	Coal Conveyor	7	Area 1	7	Second Bauxite Overflow Pad
8	Limestone Shed	8	Loadout		
9	West Conveyor	9	Pellet Bins		
10	Scrapyard	10	OHEF		
11	North Admin				
12	Quartz				

3 METHODOLOGY

An overview of the approach used in this project to monitor and analyse the stockpile volume utilising geospatial technologies is presented in this section. In order to accomplish the research goals specified in this study, a methodical approach to data collection, processing, and analysis is included in the methodology. UAVs are used in data collecting; images are processed for photogrammetric reconstruction; stockpile volume is computed; databases are created; and web-based visualisation is achieved through the use of ArcGIS technology. The approach places a strong emphasis on integrating spatial data analysis methods in order to extract valuable information from the large stockpile dataset The next sections will expound upon the procedures and instruments employed at every phase of the process, accentuating their roles in advancing the overarching research goals.

The decision to use aerial photogrammetry as the main method for calculating stockpile volume is based on realistic cost-effectiveness and operational efficiency. While LiDAR technology provides a strong alternative, providing unrivalled precision and accuracy in terrain modelling and volumetric analysis, its implementation dramatically increases both initial investment and processing costs. LiDAR systems, which rely on laser pulses for data collecting, need significant capital expenditures for purchase and deployment, making them financially prohibitive for many organisations, particularly those with limited budgets (Gaspari et al., 2022). Furthermore, the complex processing methods necessary to extract useful information from LiDAR-generated point clouds necessitate significant computer resources and time-consuming operations (Manish et al., 2022), increasing the logistical problems of timely stockpile volume reporting.

In contrast, aerial photogrammetry appears as an economically feasible and operationally simplified option that fits well with the demands of routine stockpile monitoring tasks (Mora et al., 2020). This technology, which uses photogrammetric imaging concepts, takes advantage of the inherent qualities of overlapping aerial data to generate 3D representations of landscape objects such as stockpiles. By leveraging the mobility of consumer-grade cameras installed on UAVs, aerial photogrammetry eliminates the requirement for specialised hardware expenditures, facilitating access to high-resolution spatial data capture (Alsayed et al., 2021). Furthermore, the computational needs of photogrammetric processing processes are quite low, thanks to the availability of user-friendly software solutions that accelerate the creation of DSMs and orthophoto mosaics (Adjidjonu & Burgett, 2019).

In essence, the use of aerial photogrammetry as the preferred method for stockpile volume computation exemplifies a careful balance of cost-consciousness and computational efficiency, allowing organisations to optimise resource allocation while maintaining analytical rigour in volumetric assessment efforts.

3.1 Software Used

3.1.1 Agisoft Metashape v2.0

Through the implementation of aerial triangulation, ground control integration, camera optimisation, and orthophoto production procedures, Agisoft Metashape was instrumental in turning unprocessed UAV imagery into useful geographic information. This software-driven photogrammetric workflow is an example of a data processing and visualisation approach used in stockpile volume monitoring. The key to the generation of precise models is to follow established photogrammetric procedures as explained in section 3.5.

3.1.2 Cyclone 3D Reshaper (3DR) Desktop v2023.1

Using 3DR software, the volume computation step of this project processed dense point clouds produced by Agisoft Metashape to provide stockpile volume calculations. To improve the accuracy of the volume estimates that followed, the procedure started with point cloud cleaning, in which unnecessary objects like trees and cars were systematically eliminated to leave only relevant data points related to stockpile formations. Volume computation approaches were then used in accordance with the base models that were available below the stocks. To precisely compute volume for stockpiles on pre-established base models, a 3D TIN surface of the base was created. Alternatively, a toe line was drawn at ground level to indicate the stockpile boundary for stockpiles without base models, and using the discovered ground points, an approximate ground surface model was built. This model provided the foundation for calculating the stockpile's volume using a 3D TIN model. With 3DR, these methodical processes guaranteed accurate volumetric assessments of stockpile formations.

3.1.3 AutoCAD Map 3D v2023

The stockpile footprints created with the 3DR were exported in the AutoCAD-compatible .dxf format. For geographical analysis and visualisation, this format makes seamless interaction with Geographic Information Systems (GIS) possible. In particular, the geometric properties and spatial precision of the toe lines used to demarcate stockpile footprints were preserved when they were exported as data points inside the .dxf file. The ability to process, modify, and analyse the stockpile footprints in a GIS context was made possible by exporting data in the .dxf format. The efficacy of data interchange between 3DR and GIS systems are improved by this compatibility.

3.1.4 QGIS Desktop v3.34.1

During the integration stage, the .dxf files with stockpile footprints, volumetric data, and related properties were combined using QGIS. In order to do this, the geometric representations of the stockpiles from the .dxf files had to be combined with extra data layers comprising of detailed survey information: survey date and time, surveyor details and specific material characteristics like material type, density, and moisture content. Through the use of QGIS's spatial data processing capabilities,

stockpile footprints and volumetric data from 3DR were connected, allowing for in-depth analysis and visualisation in a geographical context.

3.1.5 ArcGIS Pro v3.2.0 and ArcGIS Online

To create a comprehensive database, several layers of stockpile information were assimilated and consolidated using ArcGIS Pro, a critical tool for spatial data management. Within a single geographic framework, this geodatabase included several datasets with volumetric data, stockpile properties (such as material kind, density, and moisture), and survey information (such as survey date, location, and surveyor details). By using the extensive geospatial functionalities of ArcGIS Pro, stakeholders may arrange, examine, and represent intricate datasets, therefore promoting well-informed choices and well-thought-out strategies.

The integrated database was then used to create interactive maps in ArcGIS Pro, providing a dynamic visualisation environment for investigating and analysing stockpile inventory information. Furthermore, the dataset was distributed and shared via the ArcGIS Online platform, which allowed for increased accessibility and stakeholder participation. This distribution approach improved data accessibility and enabled remote access to vital stockpile data.

Additionally, a web application was created displaying the stockpile database in an interactive and user-friendly manner by utilising the ArcGIS Experience Builder tool. Through its integration with ArcGIS Online, the program allowed users to dynamically explore and interact with stockpile data, allowing for the real-time visualisation of survey data, attribute details, and volumetric measurements.

3.2 Datum Used

The horizontal datum used for this study is the Geocentric Datum of Australia 1994 (GDA94) which was the precursor the most recent Geocentric Datum of Australia 2020 (GDA2020). GDA94 was used as per the client requirements of data delivery. The vertical datum used in this study is Australian Height Datum (AHD) derived from AusGeoid 2009. The results of the study were presented in maps that were projected in Map Grid of Australia 1994 (MGA 1994) zone 53 projection system.

3.3 Stockpile Monitoring Workflow

In this study, the pre-existing workflow prepared by A&S for stockpile monitoring was enhanced. The improvements focus on automating data processing, development of integrated database and leveraging GIS for advanced mapping and visualization. The changes aim to enhance the efficiency of stockpile monitoring workflow. Figure 5 shows the existing methodology employed by A&S for stockpile monitoring.

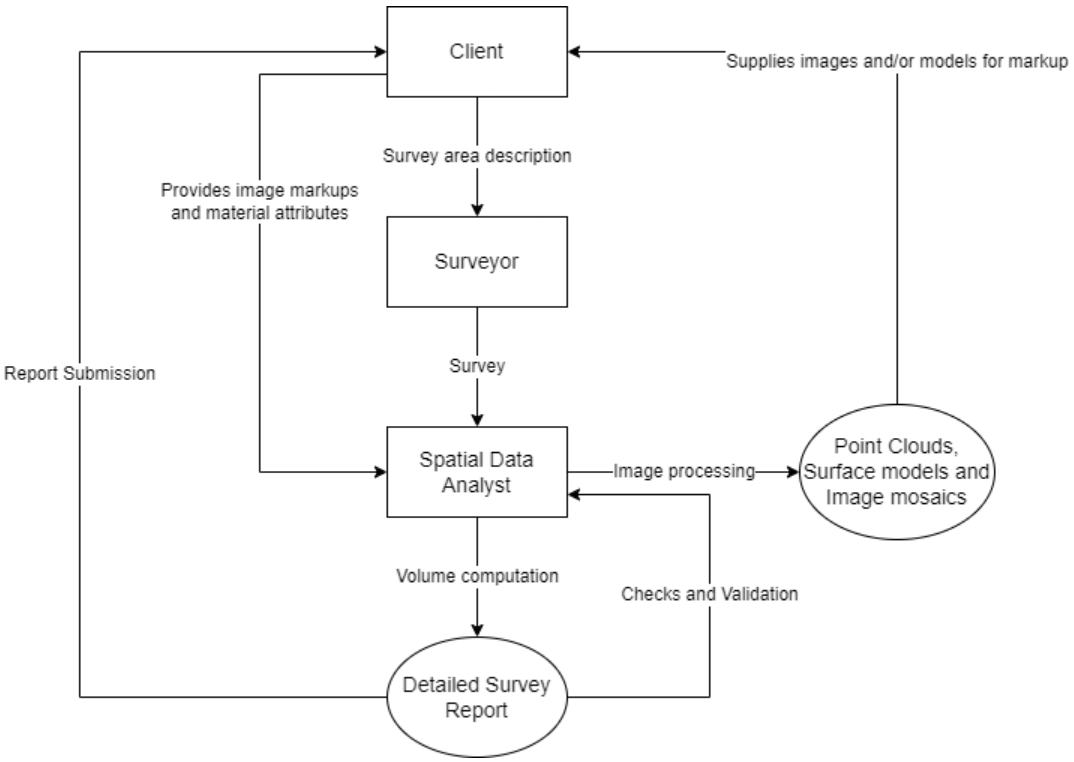

Figure 5: Existing A&S stockpile monitoring workflow

The changes made during the study are described below.

i. **Automated Extraction of Stockpile Data:** The implementation of scripts for the automatic extraction of stockpile volumes, footprint perimeter and area significantly reduced the manual effort in data processing minimizing human errors and increasing data consistency and reliability.

ii. **Integrated Database Preparation:** The preparation of an integrated database that consolidates all relevant stockpile data facilitated efficient data storage and detailed analyses. The database included temporal stockpile volumetric data, survey information and material properties.

iii. **GIS for Mapping and Visualization:** The use of GIS for tiered mapping created multi-layered maps with spatial context to stockpile data and helped in the visualization of various aspects of stockpile data. In addition, the web-based visualization provided dynamic data visualization, encouraged interactivity and provided quick access to relevant information.

Figure 6 depicts the methodological workflow implemented in this research. The following section details each of these elements.

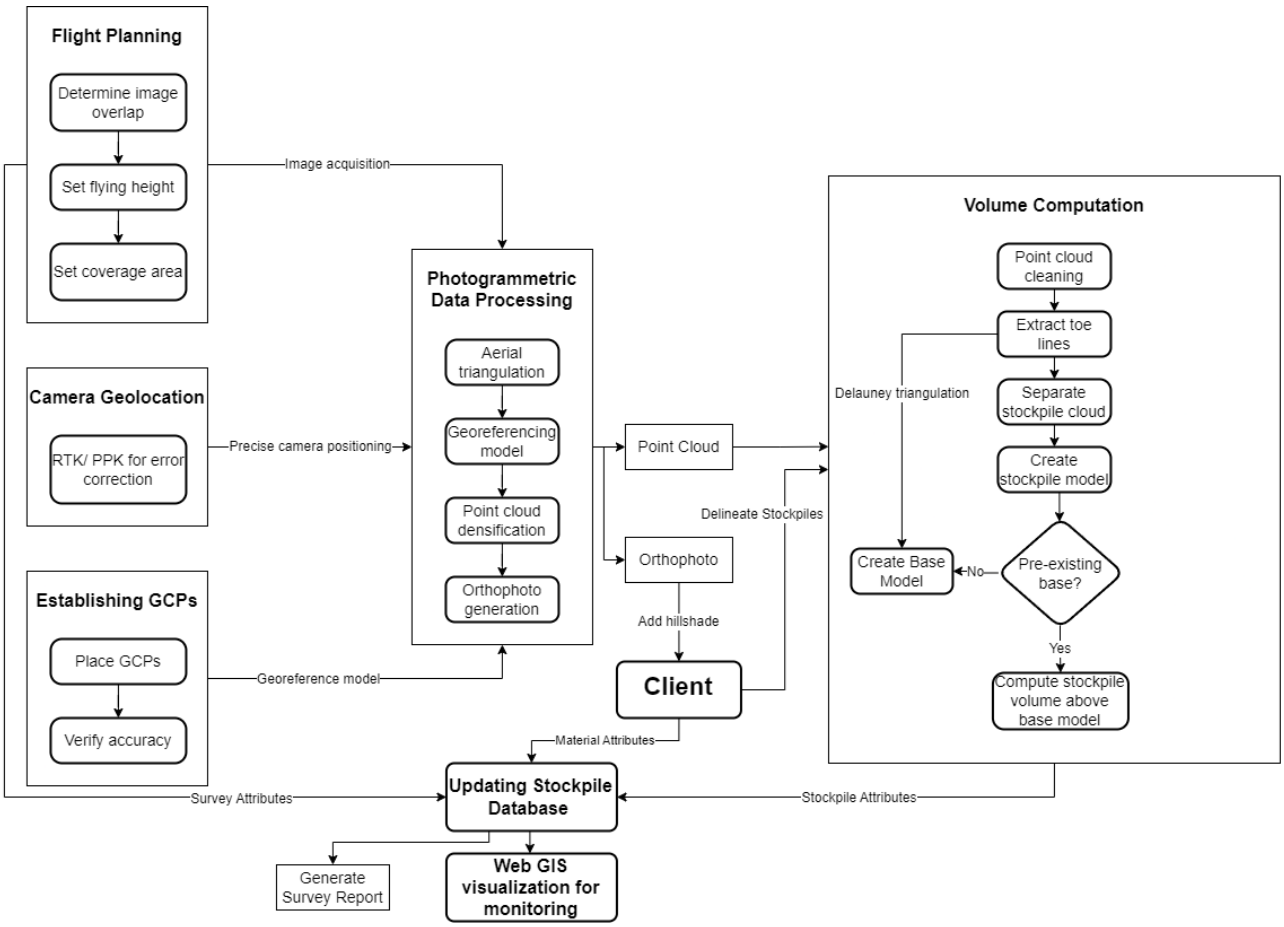

Figure 6: Methodological workflow showing steps from data acquisition to delivery

3.4 Data Acquisition

This study's data collection phase is divided into three important sub-categories: flight planning, the establishment of ground control points, and the use of PPK/RTK for accurate camera placement during image capture. Each aspect is critical to obtaining high-quality spatial data for subsequent stockpile volume computations.

3.4.1 Flight Planning

Flight planning includes considerations for image overlap, flying height, and camera selection. The degree of overlap between successive photos, along and across flight lines, is precisely calibrated to allow for robust photogrammetric reconstruction and complete coverage of the target region. Optimal flying altitudes are calculated using criteria such as desired spatial resolution, terrain complexity, and regulatory limitations. Furthermore, selecting an appropriate camera system is critical to obtaining the required picture quality and spectral integrity for accurate stockpile volume measurement. Table 3 presents the details of flight parameters used in the UAVs deployed during this project. The cameras captured nadir images with a back-and-forth flight pattern. The flight locations are presented as area of interest in Figure 7.

Table 3: UAV type, camera and flight specifications

UAV Type	DJI Phantom 4 RTK	WingtraOne Gen II
Camera	1” CMOS	Sony RX1R II
Lens	20 MP 8.8 mm lens	42 MP 35 mm lens
Flying Height (m)	120	120
Front Overlap	80%	80%
Side Overlap	70%	70%

3.4.2 Establishment of Ground Control Points (GCPs)

Ground control points are crucial reference markers for georeferencing aerial photography and minimising discrepancies between extremely precise camera positions and ground truth locations. During image processing, these precisely surveyed points are recognised within the aerial images and then used to link the photogrammetric model to real-world locations. By including GCPs into the reconstruction process, the resultant orthophoto mosaics and digital surface models achieve great spatial accuracy, increasing the dependability and precision of stockpile volume estimations.

For photogrammetric data processing and subsequent volume estimates for stockpile monitoring to be accurate and reliable, the precise placement of GCPs in the study area is crucial (Sanz-Ablanedo et al, 2019; Awasthi et al, 2019; Ferrer-Gonzalez et al, 2020). Across the research region, strategically placed GCPs act as reference points with established coordinates. The geometric precision of photogrammetric models produced from UAV imagery is greatly improved by GCPs. The relative locations and orientations of aerial photographs may be correctly calibrated by strategically placing GCPs across the research region. This reduces distortions and mistakes during the photogrammetric reconstruction process. Robust quality assurance is ensured throughout the data processing cycle by proper GCP allocation. GCPs facilitate the process of validating and adjusting photogrammetric models by offering an evaluation and mitigation mechanism for potential errors resulting from various variables such lens distortions, differences in topography, and circumstances during picture capture. Moreover, GCPs are important spatial reference points that are used to match photogrammetric data with coordinates from the ground truth. Accurate geographical analysis and interpretation of stockpile volumes are made easier by this spatial reference, which guarantees that volumetric measurements coincide with actual geographic locations. In the context of estimating stockpile volume, GCPs help to improve the accuracy and consistency of volume estimations. The production of comprehensive DSMs and elevation models, which are necessary for estimating stockpile quantities based on elevation differentials and geometric transformations, is made possible by accurate GCP placement. Furthermore, integrating UAV-derived imagery with other geospatial datasets, including satellite imagery or LiDAR data, is made easier when properly dispersed GCPs are in place. The precision and comprehensiveness of geographical studies are improved by this integration, enabling comprehensive evaluations of environmental conditions and stockpile inventories. By establishing consistent GCP networks over

time, it becomes feasible to monitor stockpile dynamics and detect volumetric changes over successive surveys. This capability is instrumental in tracking stockpile evolution, assessing material movements, and supporting decision-making processes related to resource management and operational planning. The positioning of GCPs over the study area is shown in Figure 7. These GCPs were established through GNSS survey and were monitored before each survey to ensure their accuracy. Some of the sites are missing GCPs due to the physical difficulty of the terrain and constant movement of stockpiles in the area causing erosion to physical markers.

According to Ekaso et al. (2020), DJI reports the stand-alone positional accuracy of drone to be within 2 to 3 cm and investigation with a Matrice 600 Pro utilizing RTK GNSS achieved decimeter level accuracy in direct georeferencing. RTK GNSS was enabled in the UAVs during image acquisition utilizing the nearby SmartNet ground stations. GCPs were established using RTK GNSS method with base station positioned at NAIL1 (Figure 7) to increase the accuracy of georeferencing. Shao and Yang (2016) report the accuracy of GCP established with this method to be about 2 cm enhancing the positional accuracy of the photogrammetric model.

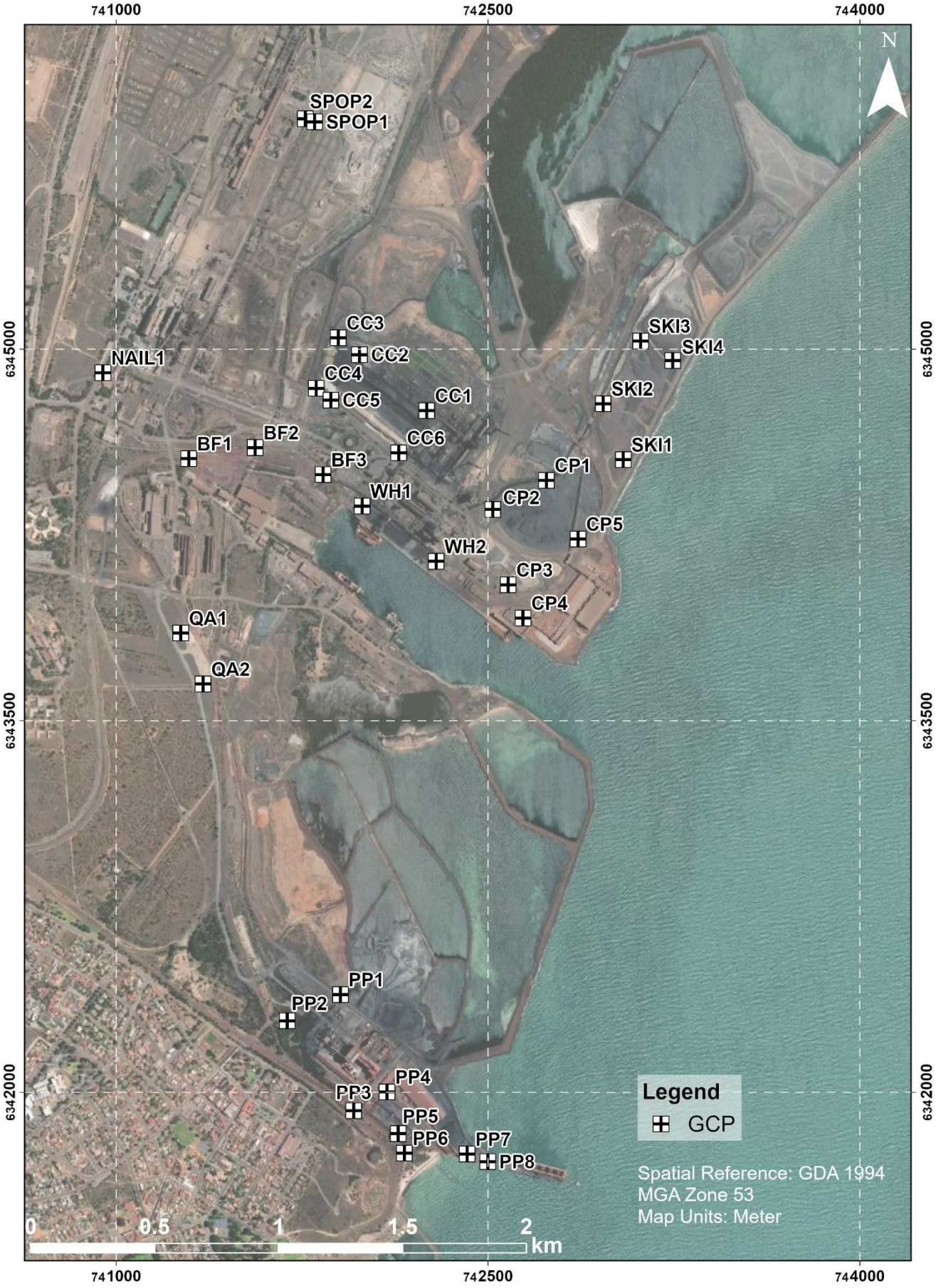

Figure 7: Image showing the distribution of GCPs in the study area.

3.4.3 Utilization of PPK/RTK for Camera Positioning

The use of Post-Processed Kinematic (PPK) or Real-Time Kinematic (RTK) positioning algorithms is critical for assuring accurate camera orientation during picture collection. PPK/RTK technology, which uses satellite-based augmentation systems (SBAS) or ground-based reference stations, allows for the extraction of very precise geolocation information for each picture captured during UAV flights. This increased positional precision not only improves the spatial integrity of the produced photogrammetric datasets, but also allows for seamless integration with ground control points, increasing the overall geometric quality of the reconstructed terrain models.

RTK technology was employed throughout this study to obtain precise camera positioning information during image capture. Nearby SmartNet bases were primarily used for RTK. In cases when the RTK signal was interrupted or dropped, SmartNet bases were used to correct the geolocation information generated from the drone's GPS measurements using PPK methods. This adaptive technique provided continuity in acquiring proper spatial reference for the aerial photos, thereby increasing the overall dependability and precision of the photogrammetric data gathering process. The difference in the two mechanisms used for generating correction values for precise camera positioning is depicted in Figure 8. RTK positioning is achieved through the real-time communication of the base station with the rover. While RTK positioning provides real-time corrections to the GPS data during the UAV flight, PPK involves recording the GPS data during the flight and applying a post-facto correction using ground-based stations (SmartNet). This methodology of precise camera positioning produced camera location error of upto 5 cm with error increasing with lower image overlapping areas in the edge of flights.

These data gathering approaches work together to enable the acquisition of high-resolution aerial photography with precise georeferencing, establishing the groundwork for reliable stockpile volume computation and analysis. Through meticulous design and implementation, the project aims to generate geographically accurate and actionable data for stakeholders in many industries that rely on stockpile management.

Figure removed due to copyright restriction

Figure removed due to copyright restriction

Figure 8: RTK v PPK correction method. Retrieved from https://www.scoutaerial.com.au/rtk-and-ppk-drone-surveys/

3.5 Photogrammetric Data Processing

During the image processing stage of aerial photogrammetry, a variety of computational approaches are used to convert raw aerial imagery into georeferenced and spatially accurate datasets suitable for volumetric analysis and visualisation. This method consists of many major processes, each of which plays a vital role in refining the obtained image and producing relevant results.

Figure 9 shows the image processing workflow employed by Agisoft Metashape which is used for photogrammetric processing in this study.

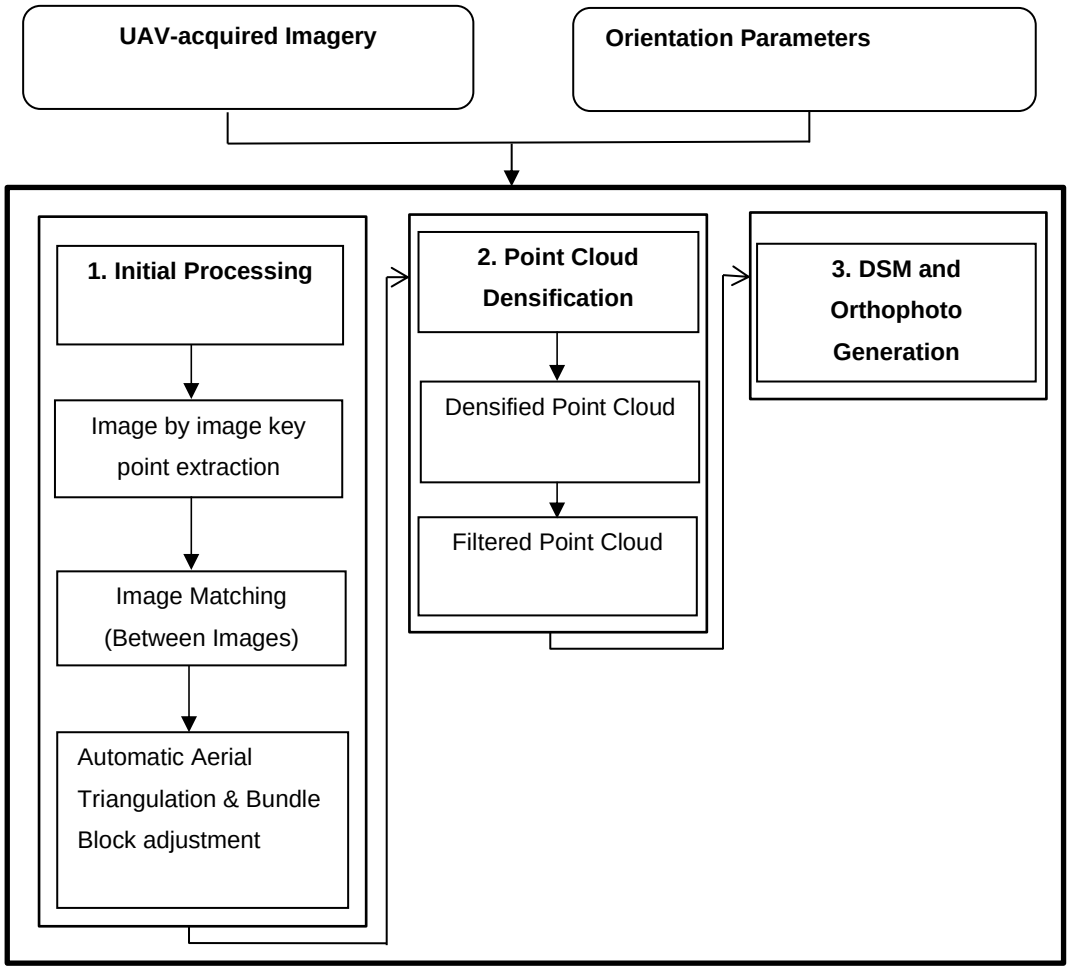

Figure 9: Photogrammetric data processing workflow in Agisoft Metashape

3.5.1 Aerial Triangulation (AT)

The first stage of image processing is called aerial triangulation, in which overlapping pictures taken from various angles are geometrically matched to provide exact relationships between image pixels and real-world coordinates. In order to facilitate the production of a coherent 3D model of the surveyed region, this approach makes use of the fundamentals of photogrammetric geometry to calculate the spatial orientation and position of each image relative to the others and the ground control points.

3.5.2 Adjustment to Ground Control

To further improve the spatial accuracy of the photogrammetric model, modifications are applied to the pre-established ground control points after aerial triangulation. By reducing disparities between the calculated and observed locations of ground control points, this iterative procedure improves the overall geometric accuracy of the rebuilt landscape. The photogrammetric models adjusted using GCPs resulted in observed model fitting error of upto 10mm.

The RMSE error obtained at GCP controlled sites in this research have been presented in Table 4. Initially, not all sites had GCPs as marked by N/A. The sites in the tab correspond to site names presented in Table 1.

Table 4: RMSE values at GCP locations for missions with ground control

		Site				
Month	**RMSE Type (cm)**	**Wharf**	**Conveyor**	**SkiRun**	**Highline**	**Plant**
Jan-2023	Avg XY RMSE	N/A	N/A	N/A	N/A	1.45
	Avg Z RMSE	N/A	N/A	N/A	N/A	1.68
	Avg Total RMSE	**N/A**	**N/A**	**N/A**	**N/A**	**2.22**
Feb-2023	Avg XY RMSE	N/A	N/A	N/A	N/A	0.72
	Avg Z RMSE	N/A	N/A	N/A	N/A	0.34
	Avg Total RMSE	**N/A**	**N/A**	**N/A**	**N/A**	**0.8**
Mar-2023	Avg XY RMSE	N/A	N/A	0.78	0.77	0.84
	Avg Z RMSE	N/A	N/A	0.47	0.61	0.67
	Avg Total RMSE	**N/A**	**N/A**	**0.92**	**0.99**	**1.08**
Apr-2023	Avg XY RMSE	1.06	3.12	0.49	0.61	0.93
	Avg Z RMSE	0.44	2.61	0.14	0.21	0.09
	Avg Total RMSE	**1.15**	**4.07**	**0.51**	**0.64**	**0.93**
May-2023	Avg XY RMSE	0.65	0.29	0.78	0.69	0.49
	Avg Z RMSE	0.02	0.05	0.34	0.12	0.44
	Avg Total RMSE	**0.65**	**0.29**	**0.85**	**0.7**	**0.66**
Jun-2023	Avg XY RMSE	0.58	0.4	1.17	1.87	1.4
	Avg Z RMSE	0.2	0.01	1.47	1.35	0.64
	Avg Total RMSE	**0.62**	**0.4**	**1.88**	**2.31**	**1.54**
Jul-2023	Avg XY RMSE	0.56	0.72	1.23	1.46	0.73
	Avg Z RMSE	3.67	0.25	1.08	1.68	0.39
	Avg Total RMSE	**3.72**	**0.76**	**1.63**	**2.23**	**0.83**
Aug-2023	Avg XY RMSE	1.67	1.57	2.27	2.14	2.74
	Avg Z RMSE	0.63	0.56	0.25	0.3	0.38
	Avg Total RMSE	**1.78**	**1.67**	**2.29**	**2.16**	**2.76**
Sep-2023	Avg XY RMSE	0.85	1.11	0.39	2.58	0.54
	Avg Z RMSE	0.23	0.42	0.17	0.42	0.24
	Avg Total RMSE	**0.89**	**1.19**	**0.43**	**2.61**	**0.59**
	Avg XY RMSE	0.67	0.31	2.09	2.45	0.59

		Site				
Month	**RMSE Type (cm)**	**Wharf**	**Conveyor**	**SkiRun**	**Highline**	**Plant**
Oct-2023	Avg Z RMSE	0.09	0.23	1.59	2.14	0.13
	Avg Total RMSE	**0.68**	**0.38**	**2.62**	**3.26**	**0.61**
Nov-2023	Avg XY RMSE	0.68	0.33	0.34	0.6	0.43
	Avg Z RMSE	0.77	0.21	0.21	0.11	0.19
	Avg Total RMSE	**0.69**	**0.39**	**0.4**	**0.61**	**0.48**
Dec-2023	Avg XY RMSE	0.56	0.26	0.44	0.48	0.34
	Avg Z RMSE	0.09	0.18	0.25	0.1	0.15
	Avg Total RMSE	**0.57**	**0.31**	**0.5**	**0.48**	**0.37**

3.5.3 Point Cloud Densification

Point cloud densification is the following step in the process, where more data points are added to the sparse point clouds created by the first photogrammetric reconstruction. This increases their point density and spatial resolution. Through this method, the point cloud representation of the landscape is enhanced in terms of detail, making it possible to delineate stockpile limits and terrain features with more accuracy.

3.5.4 Orthophoto Generation

Production of planimetrically accurate orthophotos from the perspective-distorted aerial images completes the image processing pipeline. For volumetric analysis, orthophotos provide a mathematically corrected depiction of the landscape free from perspective distortions and elevation fluctuations.

Image processing phase is a vital link between unprocessed aerial photos and useful geospatial data, providing the foundation for further analysis and understanding of stockpile volume management and monitoring. This step converts image data into accurate and coherent representations of the surveyed environment using sophisticated computer tools and iterative refinement procedures, providing stakeholders with crucial spatial information for well-informed decision-making. It provides a planimetric view of the surveyed area aiding in analyses. The orthophotos generated in this study had a resolution of 10 cm. Images of combined orthophotos produced during the study are presented in Appendix B: Combined Orthophotos.

3.6 Orthophoto Labelling

The orthophoto produced by the processed aerial data is a fundamental instrument for stockpile identification and delineation that necessitates volume calculation. at order to detect and identify the limits of individual stockpiles and start the volume calculation procedure, it is necessary to visually analyse the orthophoto at this crucial phase.

Attention to detail and a comprehensive understanding of the site's topography and stockpile attributes are necessary for the orthophoto labelling procedure. To guarantee correct identification and delineation, analysts must carefully discriminate between stockpiles and other objects or terrain characteristics visible in the data. The labelling process facilitates accurate and efficient stockpile identification for volume computation by utilising the orthophoto's extensive coverage and geographic precision.

In this study, the orthophotos were sent to clients at GFG Alliance for labelling before volume calculations started. Figure 10 shows a sample of a labelled orthophoto obtained from the client. The stockpiles are labelled with IDs which are used for providing stockpile detail in survey report.

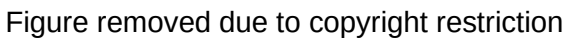

Figure 10: A sample of a labelled orthophoto for Coke Paddock

3.7 Volume Computation

Dense point clouds generated from Agisoft Metashape is used in 3DR software to precisely calculate the volume of stockpiles that have been identified. This stage consists of a few consecutive procedures, each specifically designed to extract accurate volumetric measurements and refine the point cloud data (Figure 11).

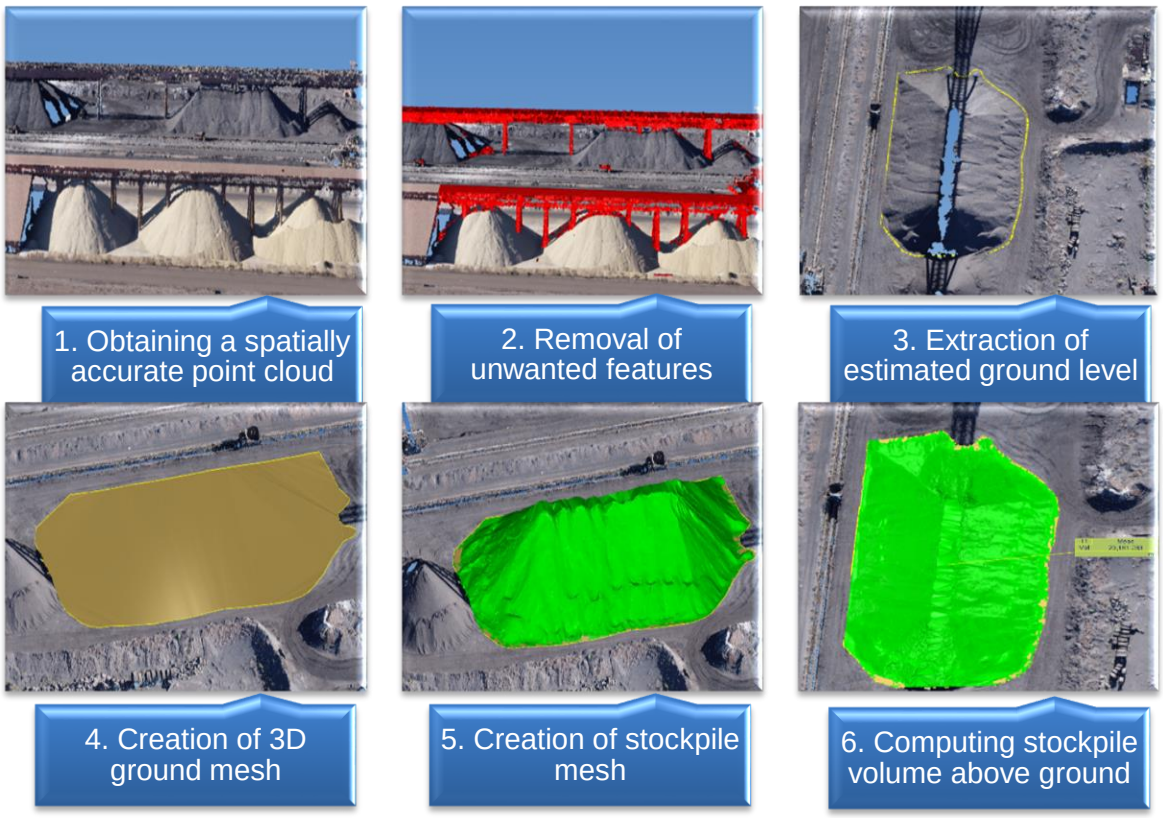

Figure 11: Overview of the stockpile volume computation process from point cloud cleaning to volume computation using 3D TINs.

3.7.1 Point Cloud Cleaning

Point cloud cleaning is the first step in volume computation, in which superfluous items like vegetation, vehicles, and overhanging conveyors are methodically eliminated from the point cloud dataset. The point cloud cleaning process employed in this methodology is completely manual. By taking great care to ensure that the volume calculations that follow are based only on pertinent data points that correspond to the stockpile formations, the accuracy and dependability of the findings are improved.

3.7.2 Stockpile Volume Calculation

The cleaned point clouds are then used as the basis for several volume computation techniques, which are contingent upon the availability of base models beneath the stockpiles. When stockpiles

are positioned on surfaces with pre-established base models, the area surrounding the base model is carefully covered by a 3D TIN surface. This makes it easier to calculate the volume above the base and gives an accurate estimate of the stockpile's volumetric extension.

On the other hand, if there are no base models available, a different strategy is used in which a toe line marking the stockpile's limit is manually extracted at ground level by joining the best identified ground points. Using the elevation information of the vertices that make up the toe line, an approximate ground surface model is created as a stand-in for the base model using constrained Delauney triangulation to generate 3D TIN surface. The volume above the assumed base may then be calculated using the 3D TIN model of the stockpile that is created over this rebuilt ground surface. This is accomplished in 3DR. After the pre-requisites of a cleaned point cloud and an existing ground base or a stand-in ground model is checked off, the volume of the stockpile formation above their respective ground model is computed in 3DR. The results of the process are organized in a directory within the project named with a unique name of the stockpile, referred to as Stockpile ID henceforth. This directory contains the following items generated by default in the 3DR software:

i. Contour: Extent of the stockpile represented by a polyline (toe line or the extents of the pre-existing ground model under the stockpile).
ii. Stockpile cloud: The point cloud of the stockpile that was used to generate the stockpile 3D TIN.
iii. Ground mesh: The 3D ground TIN or the base model.
iv. Stockpile mesh: The 3D TIN of the stockpile.
v. Label: A label providing information about the volume of the stockpile above ground.

This directory is automatically generated in the 3DR software when stockpile volumes are evaluated with a manually generated toe line. In cases where there is a pre-determined base, the directory is manually put together for organization. This directory is used as a reference for automatic extraction of stockpile footprints and volumes using javascript.

This approach produces precise measurements of the size of stockpiles as it utilizes the finely spaced 3D points (5 mm) to recreate the stockpile surface. With 3D reconstruction of a stockpile, calculations of perimeter, area and volume over selected base surface is performed. Through careful implementation of these procedures throughout the volume computation stage, precision of the geometric attributes of the stockpile is ensured.

3.8 Creation of Stockpile Database

A key component of this research is the establishment of an extensive stockpile database, which will function as a clearinghouse for vital characteristics and volumetric measurements obtained from the volumetric analysis of stockpile formations. In the study's temporal framework, which runs from

January 2023 – December 2023, every survey that is completed results in a geographically referenced database entry that contains relevant information that is necessary for inventory management and decision-making procedures.

The stockpile database's features comprise a wide range of metrics that are crucial for describing and measuring stockpile stocks. These characteristics, which offer basic geometric descriptors of the geographical extent and footprint of the examined stockpiles, comprise the perimeter and two-dimensional area of each stockpile formation. Additionally, volumetric measurements—which include the entire volume of each stockpile—provide crucial information on the amount of material build-up at the determined sites, supporting efforts related to resource allocation and strategic planning.

The database includes the date of each survey and the name of the surveyor in charge of gathering and processing the data. Stakeholders may follow changes in stockpile levels over time using this temporal context, which allows for trend analysis and performance evaluations. Additionally, each stockpile site's name and position are included in the database, which enables spatial queries and analyses of stockpile distributions amongst different operating locations. Furthermore, the database contains material-specific information such as the name and density of the stockpile material, providing details about the make-up and features of the stockpiles under study.

The database is prepared using the following information tables:

i. A stockpile volume calculation directory (in 3DR) as mentioned in section 3.7.2 which is a resultant of the stockpile volume calculation process.
ii. Scripts for extraction of stockpile volume and footprint polyline. This was prepared to expedite the creation of stockpile information database (refer to Appendix A: Scripts used in methodology).
iii. A GIS sites layer containing the geometry and names of stockpile site locations. These are the sites presented in the study map (refer to
iv. Figure 4).
v. Survey metadata table containing site name, survey datetime, survey method and surveyor name. This information is provided by the aerial survey team.
vi. Stockpile ID information table containing stockpile ID and its corresponding material name. This is provided by the client during the orthophoto labelling phase.
vii. Material information containing material name and its attributes (density and moisture). This is a specifications sheet provided by the client and is updated when changes are recommended.

Firstly, the JavaScript “extract poyline.js” is run to extract all the footprints of the stockpiles in a .dxf format for each site. These .dxf files only contain the geometry of the footprints which are

each placed in a CAD layer with their Stockpile ID as the layer name. Then, the javascript “stockpile volume to csv.js” is run to extract the stockpile volumes in a csv format corresponding to their Stockpile ID. The multiple .dxf files for each site are merged in GIS and subsequently joined with the volumes to initialize the Stockpile Information database. This layer has Stockpile ID, stockpile volume and the footprint geometry as its attributes.

Furthermore, steps are taken to add more attributes to the GIS layer which is shown in Figure 12.

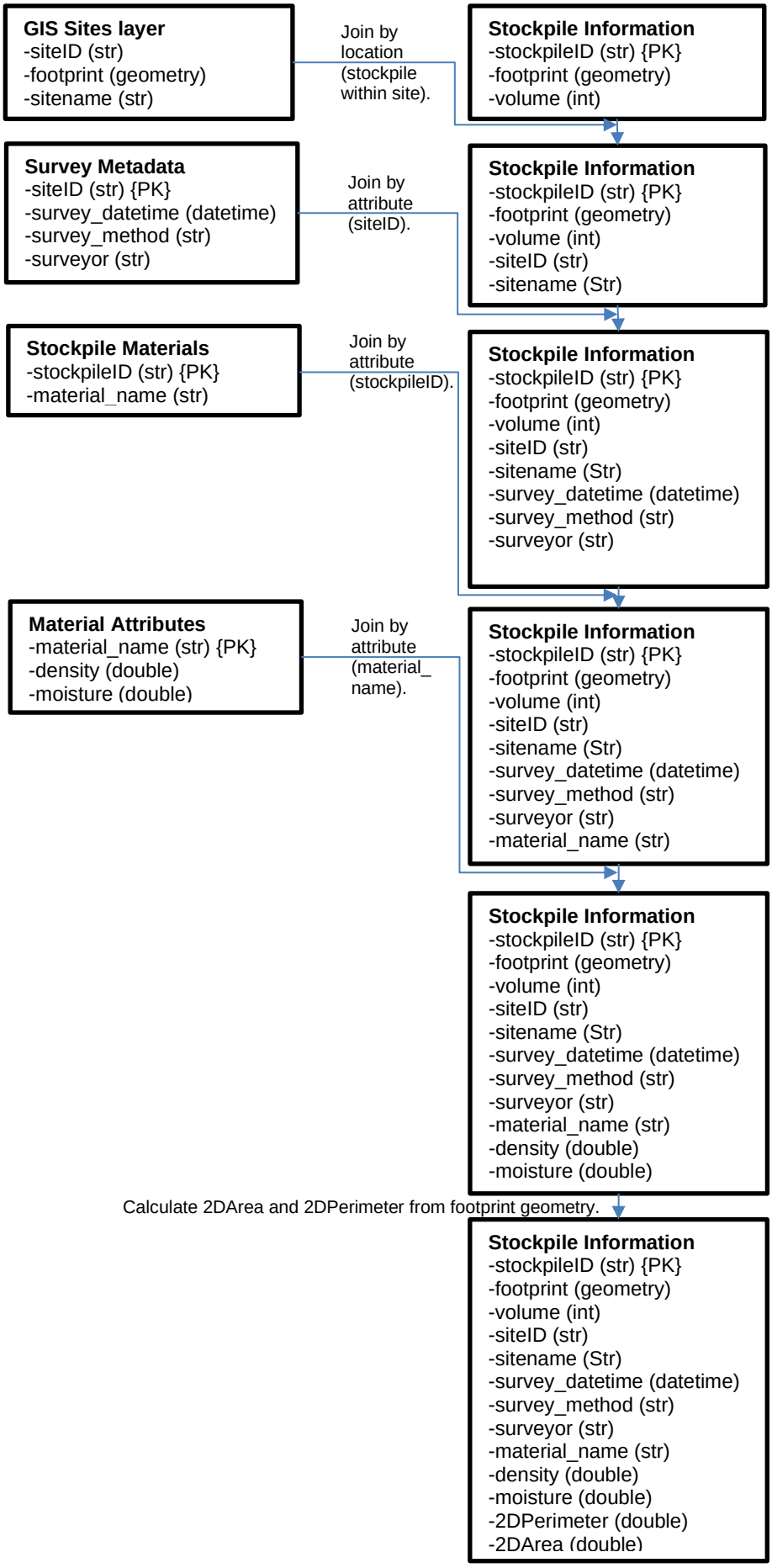

Figure 12: Steps for the creation of stockpile information database

Furthermore, the database makes it simpler to calculate the total dry and wet tonnage for every stockpile by using the numbers for density and moisture content to provide precise estimations of material tonnages. Stakeholders may evaluate resource availability and streamline material handling and transportation processes with the use of this information, which is crucial for inventory management and logistical planning. Mathematically,

$$Dry\ Tonnage(Dtns) = Volume(m^3) * Density\ (tns/m^3)$$

$$Wet\ Tonnage(Wtns) = Dtns * (1 + Moisture)$$

Where Moisture is the amount of moisture in a stockpile material.

After the addition of the calculated fields dry tonnage and wet tonnage in the database, the database is complete. The attributes of this layer and the corresponding data type is presented in Table 5.

Table 5: Attributes of the stockpile information database

Attribute Name	Data Type
StockpileID	String
Footprint	Geometry
Volume	Integer
SiteID	String
SiteName	String
Survey_Datetime	Datetime
Survey_Method	String
Surveyor	String
Material_Name	String
Density	Double
Moisture	Double
2DPerimeter	Double
2DArea	Double
DryTonnage	Double
WetTonnage	Double

This description accounts for the compilation of a comprehensive database for one survey period. Finally, data from every month was put together in one layer for use in visualization.

Overall, the endeavour to compile and arrange volumetric data obtained from aerial photogrammetry surveys carried out in 2023 is reflected in the establishment of the stockpile database. The database provides stakeholders with actionable insights into stockpile inventories by encapsulating key attributes and volumetric measurements within a spatially referenced framework. This enables informed decision-making and resource management strategies within the operational context of the study.

3.9 Web based visualization

Utilising the extensive stockpile information database, the ArcGIS web experience was developed as part of the web-based visualisation process. This involved creating dynamic and interactive web maps that were customised for the three projects: Iron Making, Pellet Plant and Steel Making. Users of this online application are able to examine stockpile data from various months and places through the use of clear visualisations owing to the incorporation of temporal and geographical aspects.

One of the online application's primary features is a timeline tool that lets users browse through monthly stockpile data, making temporal analysis and trend detection easier. Two interactive bar graphs that visualised stockpile quantities categorised by location and material type are also included. These graphs offered useful summaries of the composition and distribution of stockpiles. Pop-up windows, which enhanced data exploration and understanding by displaying summary information about individual stockpiles upon interaction, are an essential part of the application. Additionally, a dynamic table was included to display specific details about the stockpiles that can be seen on the map extent, providing in-depth understanding of each stockpile's attributes.

To enable real-time quantification and evaluation of stockpile stocks, the application also included a text box feature that dynamically updated to show the entire volume of stockpiles within the visible map extent. This interactive functionality ensured that any changes in map extent or user interactions instantly updated the displayed information, maintaining data accuracy and relevancy throughout the exploration process.

Altogether, the ArcGIS web experience demonstrated a well-developed platform for the analysis and visualisation of stockpile data, offering stakeholders user-friendly tools for exploring, navigating, and interpreting volumetric data over several projects and temporal dimensions. The importance of geospatial technology in supporting data-driven decision-making and operational insights in the fields of stockpile management and resource planning is highlighted by this dynamic and user-centric approach to web-based visualisation.

4 RESULTS AND ANALYSES

In this section, the results of data obtained by UAV photogrammetry and volumetric calculations carried out in 2023 is presented. This main goal of the analyses is to drive important information on stockpile measurements, material distributions, and temporal fluctuations from the selected project sites: Iron Making, Pellet Plant and Steel Making (Figure 4). As per the objectives set, a methodology for stockpile volume computation is detailed in section 3. The methodology was utilized for the monthly stockpile volume computation over the study period resulting providing the means of robust monitoring. The insertion of the monthly datasets into the stockpile geodatabase led to a comprehensive stockpile database for the year 2023. To guarantee data quality and consistency across all dimensions, the datasets underwent rigorous preparation before analysis, including data cleaning, transformation, and integration. The transition of stockpile volume reporting from spreadsheet-based reporting to tiered maps and web-based visualization is presented in this section. The enhanced reporting and visualization capabilities with the use of ArcGIS Online has been summarized in this section. Additionally, the stockpile database has facilitated the stockpile volume change analysis and the examination of existing patterns in the monthly stockpile volume data based on storage locations and material types.

4.1 Reporting

4.1.1 Traditional Reporting Methods in Spreadsheets

One of the objectives of this study was to modernize the reporting process. The existing reporting process involved submitting tabular data about surveyed stockpile information, material attributes and computed stockpile dimensions and resulting tonnage based on provided density in a spreadsheet with pictorial representation of surveyed sites. Table 6 shows a traditional table with stockpile survey information for the Coal Conveyor site under the Iron Making Project and Figure 13 shows its corresponding pictorial representation in a separate sheet for the December survey.

Table 6: An example of survey reporting using spreadsheets

ID	Survey Time	Survey Date	Survey Type	Material	Location	Volume (m^3)	Density (tns/m^3)	Moist (%)	Tonnage (Dry)	Tonnage (Wet)
1301D	1220	18/12/2023	Aerial	BLENDED COAL	COAL CONVEYOR	3551	-	-	INSUFFICIENT DATA	INSUFFICIENT DATA
1306	1220	18/12/2023	Aerial	BLENDED COAL	COAL CONVEYOR	5710	-	-	INSUFFICIENT DATA	INSUFFICIENT DATA
1307	1220	18/12/2023	Aerial	BLENDED COAL	COAL CONVEYOR	4016	-	-	INSUFFICIENT DATA	INSUFFICIENT DATA
1309A	1220	18/12/2023	Aerial	ALPINE COAL	COAL CONVEYOR	2860	0.86	0.110	2,460	2,730
1401C	1220	18/12/2023	Aerial	IMPORT COKE	COAL CONVEYOR	49098	0.50	0.070	24,549	26,267
1820	1220	18/12/2023	Aerial	LIMESTONE LUMP	COAL CONVEYOR	2147	1.46	0.005	3,135	3,150
WASTE	1220	18/12/2023	Aerial	WASTE	COAL CONVEYOR	675	-	-	INSUFFICIENT DATA	INSUFFICIENT DATA

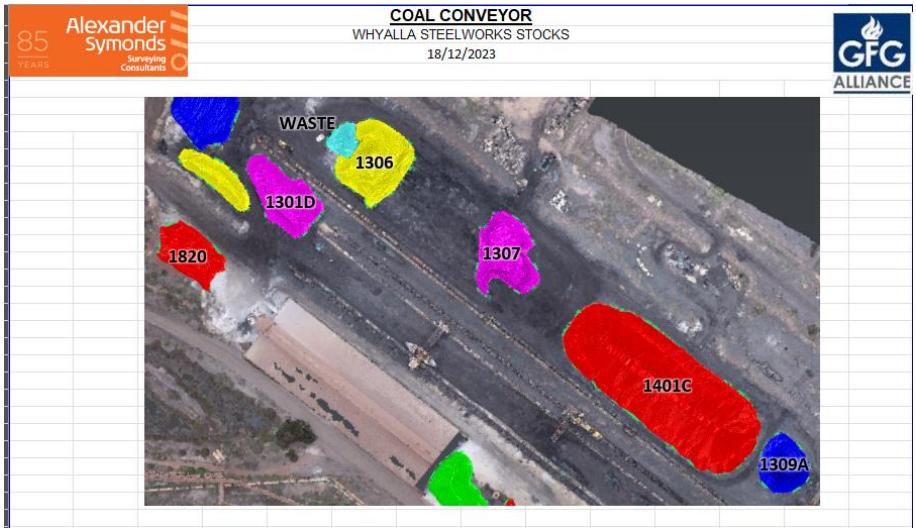

Figure 13: A pictorial representation of the stockpile location.

4.1.2 Monthly Reporting using Maps

Maps were introduced in order to improve the monthly reporting techniques. A system of 3 tiered maps (Figure 14, Figure 15, Figure 16) were presented to provide a thorough visualization of stockpiles and their associated attributes consisting of a stand-alone overview plan, an atlas of location index plan showing each sub-site and an atlas of stockpile volumes plan presenting detailed information for each stockpile.

Overview Plan: An overview plan provides a high-level view of the entire site showing all sub-sites and stockpiles and is useful in identification of the areas of interest or concern (Figure 14).

Location Index Plan: A location index plan is prepared for every sub-site within a project allowing a more detailed inspection of stockpiles within each sub-site. This facilitates sub-site level reporting and localizes information (Figure 15).

Stockpile Volumes Plan: A stockpile volume plan is prepared for every surveyed stockpile depicting survey attributes, material attributes, stockpile dimensions and computed tonnage. This allows for ease of tracking of each stockpile and fosters simpler change and trend analysis. (Figure 16).

This reporting strategy aims to enhance efficiency, accuracy and usability aiding in stockpile data management and providing better insights for strategic planning.

Figure removed due to copyright restriction

Figure 14: An example of an overview map for Iron Making in December 2023

Figure removed due to copyright restriction

Figure 15: An example for a location index plan for Coal Conveyor in December 2023

Figure removed due to copyright restriction

Figure 16: An example of stockpile volume plan for stockpile ID 1309A in December 2023

4.1.3 Online Reporting and Monitoring using ArcGIS Online

Although tiered maps present a detailed information of monthly stockpile status, it is merely a static representation of data. The use of an online platform such as ArcGIS Online provides improved ways of data visualization and analysis. To demonstrate this, a web application was built using ArcGIS Web Experience Builder which allows for interactive visualization and dynamic data representation with a user-friendly interface.

The components of the web maps are described in Figure 17.

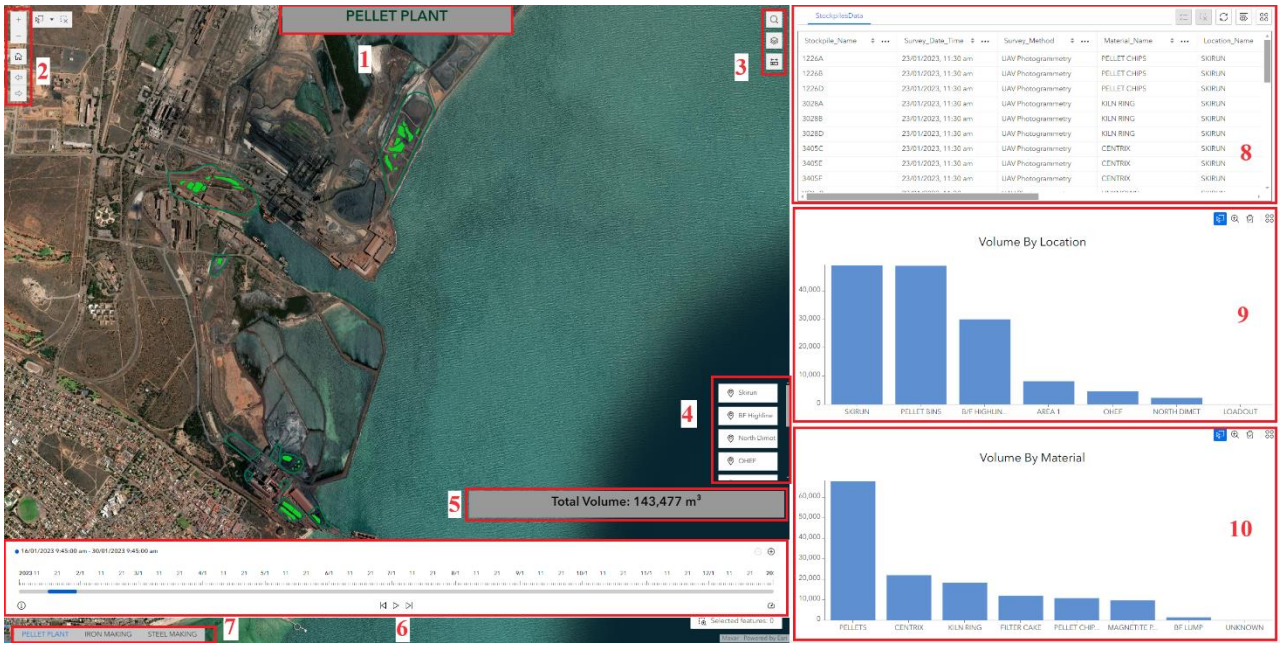

Figure 17: Web based stockpile viewer application with different components numbered from 1 to 10. The key to the labelled components is provided in Table 7

Table 7: Description of the web application components.

Component Number	Description
1	Title of the web map.
2	Map navigation tools.
3	Additional map tools: search, layer switcher and measure.
4	Bookmarks of sub-sites.
5	Total volume accumulation.
6	Timeline switcher.
7	Project switcher.
8	Detailed table of stockpiles in visible extent.
9	Dynamic bar graph representation total volume of stockpiles in sub-sites
10	Dynamic bar graph representation total volume of stockpiles based on materials.

With the introduction of a web-based dynamic mapping platform, the end-users can interact with the maps for relevant information. This is achieved using the navigational tools (Component 2 in Table 7) presented in Figure 17 permitting panning and zooming at necessary viewing scales. Additionally, each sub-site can be quickly accessed with the help of bookmarks (Component 4 in Table 7). The total volume accumulation is quickly observable through Component 5 in Table 7 and is dynamically updated to reflect the visible features in the map. The project switcher (Component 7 in Table 7) enables switching to different projects and saves the last selected state of the prior view. The table (Component 8 in Table 7) provides a detailed description of each feature in the map and the charts (Component 9 and 10 in Table 7) provide stockpile information based on location and material type. Moreover, a summary information for each stockpile each generated using a pop-up upon clicking (Figure 18).

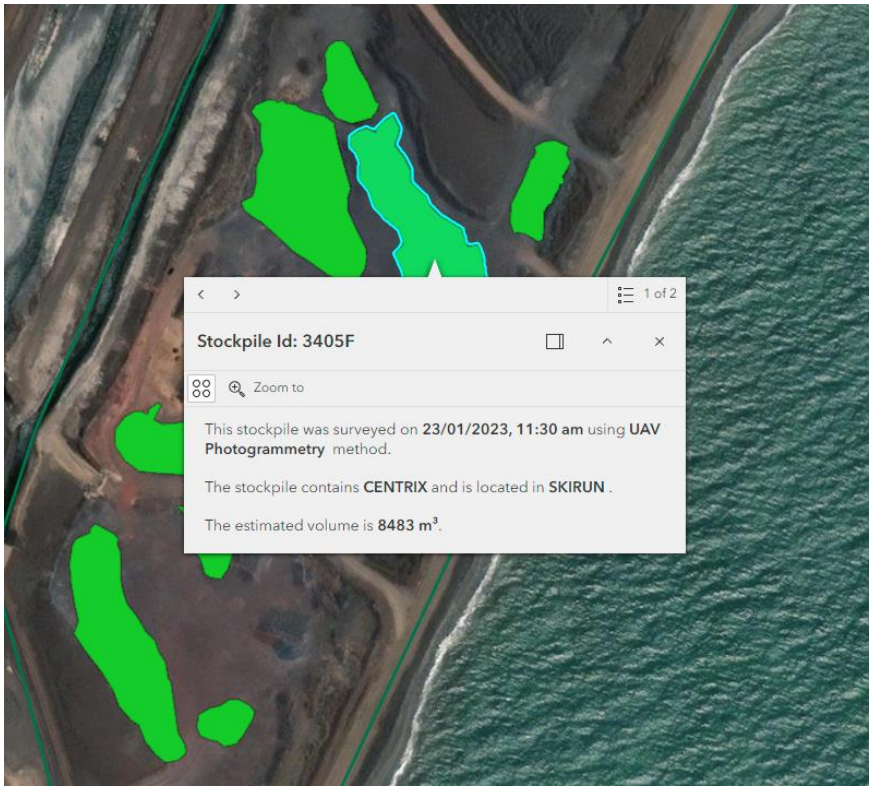

Figure 18: Stockpile summary using a click enabled pop-up.

The charts and tables in the application are integrated to dynamically respond to changes in the map extent and the timeline bar which enables efficient visualization of information in selected spacetime. The monthly changes in stockpiles can be easily visualized using the timeline bar which dynamically updates all the map components (Figure 19).

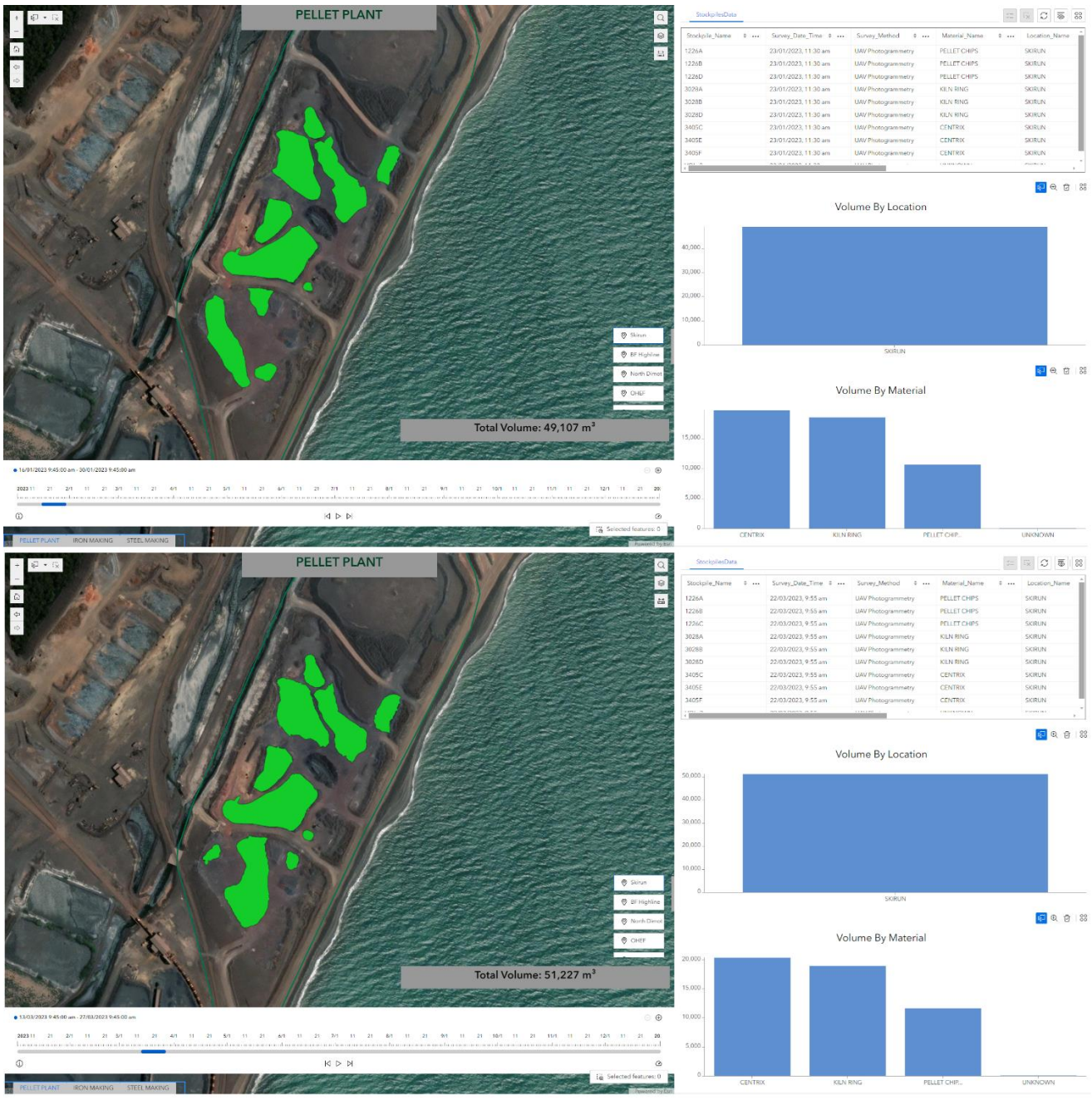

Figure 19: Dynamic changes in map components with timeline change from January to March

Figure 20 shows the dynamic changes in all map elements with the change of map extent. In the press of a button, the details for sub-sites can be generated using the help of bookmarks or a user can select multiple sub-sites which will aggregate the information presented in map extent to include all visible stockpiles.

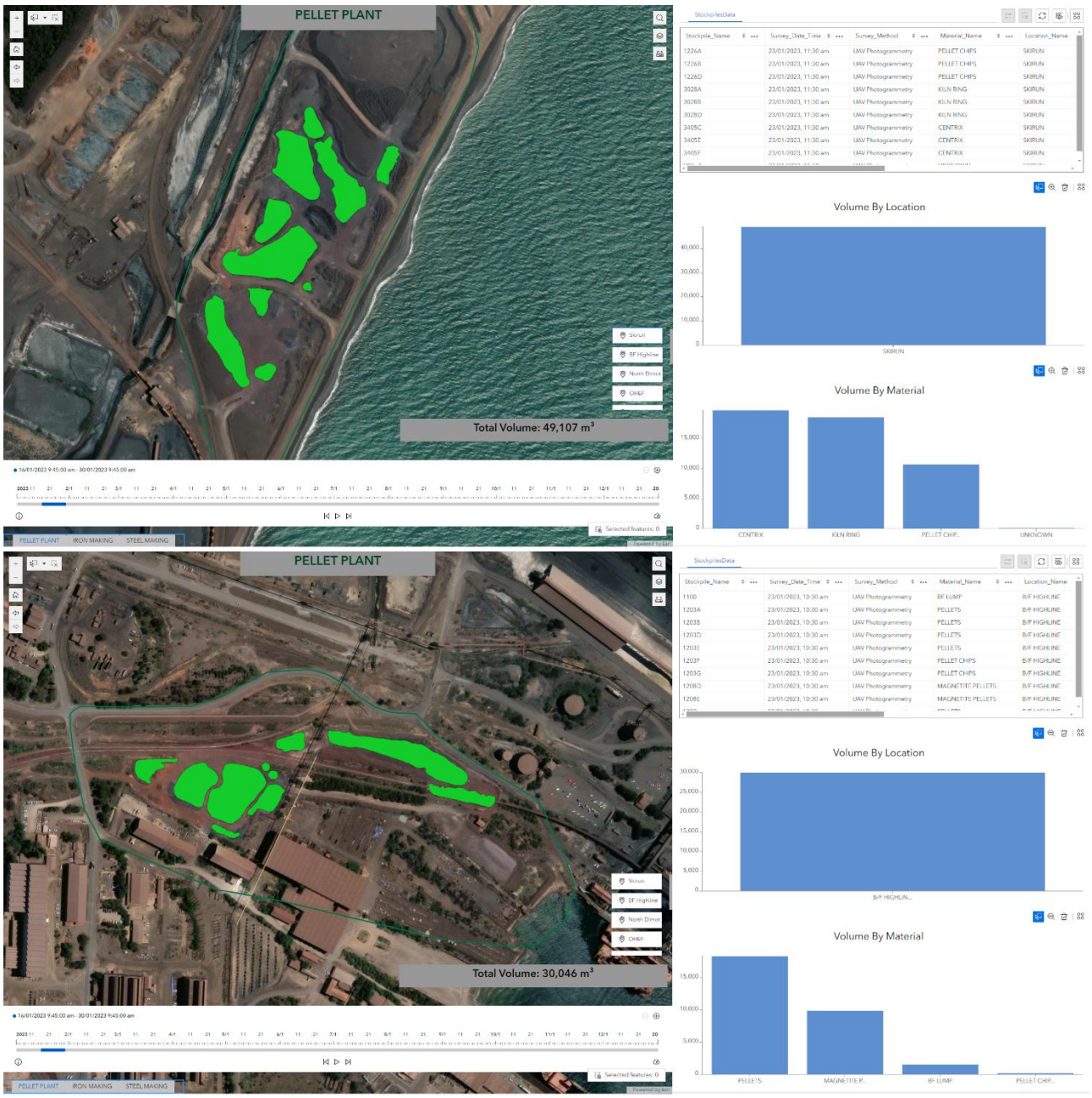

Figure 20: Dynamic changes in map components with map extent changes from Skirun to BF Highline area.

The tables and charts allow for further exploration with the help of several tools and filters. The data can be summarized for key statistics or exported to json, geojson or csv formats (Figure 21). The selected data in table can also be located in maps for visualization. Similarly, filters can be set on the rows and columns allowing a granular analysis of stockpiles.

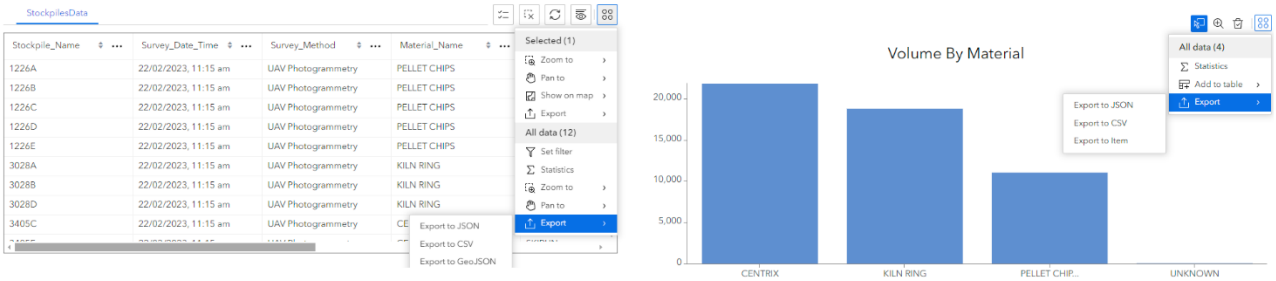

Figure 21: Table and chart tools for interaction with data equipped with filters and export options.

4.2 Change Analyses

4.2.1 Changes in Stockpile Count

A total of 1365 stockpiles were surveyed across 29 sites under three projects during the time period. Variations can be observed in the number of stockpiles surveyed at each site. Table 8 offers an overview of the stockpile surveys that were carried out at sites throughout various months of 2023. The survey months are shown along the columns and the site names are presented along the rows in the table's layout. The number of stockpiles assessed at each site for the corresponding month is shown by each cell in the table and are sectioned to show the overview for each project.

Table 8: A summary of the number of stockpiles surveyed at selected sites by month.

SITES	Jan	Feb	Mar	Apr	May	Jun	Jul	Aug	Sep	Oct	Nov	Dec	Grand Total
IRON MAKING	**66**	**66**	**60**	**67**	**61**	**60**	**55**	**57**	**54**	**54**	**43**	**53**	***696***
AMMONIUM SULPHATE SHED	2	2	2	2	1	1	1	2	2	2	2	1	*20*
CO RESERVE	2	2	2	1	2	1	1		1				*12*
COAL CONVEYOR	6	6	6	6	6	7	7	5	5	5	1	7	*67*
COKE PADDOCK	25	26	22	32	25	26	22	32	32	32	26	23	*323*
COKE PADDOCK SOUTH												2	*2*
LIMESTONE PAD	5	4	4	4	4	4	4	4	4	4	4	4	*49*
LIMESTONE SHED	2	2	1	1	1	1	1	1	1	1	1	1	*14*
NORTH ADMIN	4	4	4	3	4	4	4	4	1	1	1	1	*35*
QUARTZ AREA	4	4	4	4	4	4	5	5	4	4	4	4	*50*
SCRAP YARD	3	4	4	4	4	3	3	3	3	3	3	3	*40*
SLAG	4	3	3	3	3	2							*18*
SOUTH SCRAP YARD			2	2	2	1	1						*8*
WEST CONVEYOR	4	4	5	4	4	4	4					5	*34*
WHARF	5	5	1	1	1	2	2	1	1	2	1	2	*24*
PELLET PLANT	**35**	**35**	**40**	**38**	**37**	**34**	**31**	**38**	**38**	**36**	**32**	**33**	***427***
AREA 1	7	6	9	7	8	7	4	7	9	5	5	5	*79*
B/F HIGHLINE	10	9	12	10	10	10	8	11	10	11	10	10	*121*
FILTER PLANT			1	1	1		1	1	1	1		1	*8*
LOADOUT	2	2	2	3	2	1	2	3	2	3	2	2	*26*

SITES	Jan	Feb	Mar	Apr	May	Jun	Jul	Aug	Sep	Oct	Nov	Dec	Grand Total
NORTH DIMET	2	2	2	2	2	2	2	2	2	2	1	1	*22*
OHEF	1	1	1	1	1	1	1	1	1	1	1	1	*12*
PELLET BINS	3	3	3	3	3	3	3	3	3	3	3	3	*36*
SKIRUN	10	12	10	11	10	10	10	10	10	10	10	10	*123*
STEEL MAKING	**23**	**23**	**22**	**22**	**22**	**21**	**22**	**17**	**17**	**17**	**17**	**19**	***242***
BIS BINS	3	3	3	3	3	3	3	3	3	3	3	3	*36*
LIMEKILN	2	3	3	3	3	3	3	3	3	3	3	3	*35*
LIMESTONE PAD	1	1	1	1	1	1	1	1	1	1	1	1	*12*
OSPB	7	6	5	5	5	4	5	5	5	5	5	5	*62*
REFACTORY WAREHOUSE	5	5	5	5	5	5	5	5	5	5	5	5	*60*
SECOND BAUXITE OVERFLOW PAD	2	2	2	2	2	2	2					2	*16*
STEEL PRODUCTS OVERFLOW PAD	3	3	3	3	3	3	3						*21*
Grand Total	**124**	**124**	**122**	**127**	**120**	**115**	**108**	**112**	**109**	**107**	**92**	**105**	***1365***

21 of the 29 sites under observation conducted monthly stockpile surveys over the year. There seems to be very little temporal diversity between these locations although there are a few noteworthy outliers, such as Coke Paddock within Iron Making, Area 1, and B/F Highline within Pellet Plant. Just 7 out of 29 locations had an average of more than 5 stockpiles inspected each month. Amongst these, Coal Conveyor (29%) and Area 1 (24.5%) had a high value for coefficient of variation (CV) indicating significant dispersion from mean in the total number of stockpile counts.

When project-level trends were taken into account, Iron Making showed the largest average number of stockpiles surveyed each month (58) with a survey count CV (12%). With a CV of 7.5%, Pellet Plant averaged 35.5 stockpiles every month, whereas Steel Making averaged 20 stockpiles per month with the highest survey count CV of 12.5%.

The quantity of stockpiles measured exhibited an overall decline in all three projects. The highest number of stockpiles inspected (127) was in April, while the lowest count (92) was in November. These patterns draw attention to variations in survey activity over time within each project, suggesting possible changes in operational priorities or seasonal differences in attempts to monitor stockpiles.

4.2.2 Changes in Stockpile Volume Based on Location

Upon analysing the stockpile volume data, significant patterns and trends emerge that offer valuable insights into the processes of stockpile buildup in the research region. Notable variations in average stockpile volumes and variability (measured using CV) is explained on the basis of the data summarized in Table 9. The volumes here are expressed in cubic meters (m^3).

Table 9: A summary of the total volume of all stockpiles surveyed at selected sites by month.

SITES	Jan	Feb	Mar	Apr	May	Jun	Jul	Aug	Sep	Oct	Nov	Dec	*Grand Total*
IRON MAKING	**292495**	**314440**	**312761**	**255788**	**266393**	**263773**	**231692**	**211272**	**241727**	**160820**	**95957**	**190879**	***2837997***
AMMONIUM SULPHATE SHED	926	720	856	541	584	772	578	391	370	296	270	224	*6528*
CO RESERVE	3325	4414	2116	2826	3769	1082	615		2464				*20611*
COAL CONVEYOR	73574	103503	92697	63790	89754	89929	63559	70594	72660	29233	5092	68057	*822442*
COKE PADDOCK	106762	115624	109792	96575	71777	73197	74334	78371	100458	75732	35745	34339	*972706*
COKE PADDOCK SOUTH												15190	*15190*
LIMESTONE PAD	26568	27983	36199	24231	35594	38094	34062	26208	35217	24057	17026	15273	*340512*
LIMESTONE SHED	22298	19598	27311	25387	18399	16772	12371	11392	18891	13191	11515	23839	*220964*
NORTH ADMIN	5176	4450	2927	2261	2005	4021	7252	6414	429	866	1355	2918	*40074*
QUARTZ AREA	6912	6118	5124	5102	5375	4933	4894	3761	2769	3355	3005	4646	*55994*
SCRAP YARD	1222	2017	2769	3148	3396	3235	3583	4340	4793	4921	5252	5185	*43861*
SLAG	4267	12233	19556	18442	23767	9770							*88035*
SOUTH SCRAP YARD			1882	997	574	450	436						*4339*
WEST CONVEYOR	8959	9098	9424	8856	8867	8832	8944					11609	*74589*
WHARF	32506	8682	2108	3632	2532	12686	21064	9801	3676	9169	16697	9599	*132152*
PELLET PLANT	**143477**	**155811**	**182517**	**168035**	**146155**	**165796**	**150536**	**122875**	**122413**	**126939**	**118995**	**148095**	***1751644***
AREA 1	8244	1410	16136	26557	25751	23155	22202	31752	10777	9842	22583	41700	*240109*
B/F HIGHLINE	30046	27622	29285	26515	21971	20321	14205	10901	8796	14580	13129	11451	*228822*
FILTER PLANT			1153	607	989		4	511	184	303		755	*4506*
LOADOUT	28	67	103	442	102	7	97	77	392	12	109	111	*1547*
NORTH DIMET	2393	2399	2379	2611	2629	2613	2649	2637	2617	2834	2688	2630	*31079*
OHEF	4736	23530	27537	12113	13380	23979	18356	11687	30088	8023	14073	30070	*217572*
PELLET BINS	48923	48838	54697	60000	40169	51370	47580	19335	23637	43487	38469	32971	*509476*
SKIRUN	49107	51945	51227	39190	41164	44351	45443	45975	45922	47858	27944	28407	*518533*
STEEL MAKING	**2846**	**3236**	**2634**	**2481**	**2113**	**2341**	**2773**	**2407**	**2544**	**2568**	**2335**	**2705**	***30983***
BIS BINS	513	1088	838	729	541	869	765	524	757	919	715	731	*8989*
LIMEKILN	270	260	186	302	215	282	320	284	294	325	387	503	*3628*
LIMESTONE PAD	602	886	795	714	621	558	977	911	930	836	674	667	*9171*
OSPB	1092	617	387	321	355	360	438	530	406	332	401	561	*5800*
REFACTORY WAREHOUSE	159	157	157	156	158	156	159	158	157	156	158	158	*1889*
SECOND BAUXITE OVERFLOW PAD	39	38	46	37	29	20	21					85	*315*
STEEL PRODUCTS OVERFLOW PAD	171	190	225	222	194	96	93						*1191*
Grand Total	**438818**	**473487**	**497912**	**426304**	**414661**	**431910**	**385001**	**336554**	**366684**	**290327**	**217287**	**341679**	***4620624***

The average stockpile volume in the Iron Making project is found to be significant at 236,500 m^3, with a 27% coefficient of variation. This indicates a substantial build-up of stockpile material but there has been a notable fluctuation in volume measurements over time. Likewise, the Pellet Plant project displays a sizable average stockpile volume of 145,970 m^3 together with a comparatively low coefficient of variation (14%), suggesting more stable volume measurements during the course of the study. By comparison, the Steel Making project has smaller average stockpile volumes, averaging 2,582 m^3 with an 11% coefficient of variation indicating lower volume accumulation than Iron Making or Pellet Plant alongside less unpredictability.

With average volumes of 68,536 m^3 and 81,059 m^3, respectively, the research notably highlights the two main sites—Coal conveyor and Coke paddock—as the largest contributors to stockpile volume buildup. Higher coefficients of variation (40% and 33%, respectively) are also present at these sites, suggesting more noticeable variations in stockpile volumes over time.

The stockpile volume monitoring in the Refactory Warehouse site under Steel Making showed very little change throughout the study period with a C.V. of only 1%. This implied that there has been no material change at the site which was corroborated by the clients upon further investigation.

Figure removed due to copyright restriction

Figure 22: Monthly stockpile volume changes by site in Iron Making; A shows sites with high volume accumulation and B shows sites with low volume accumulation.

Figure removed due to copyright restriction

Figure 23: Monthly stockpile volume changes by site in Pellet Plant

Figure removed due to copyright restriction

Figure 24: Monthly stockpile volume changes by site in Steel Making

Similar to the monthly trend of total stockpile count, the volume buildup also shows a declining trend in all three projects. March (497912 m^3) had the highest reported stockpile volume accumulation while November (217287 m^3) was the lowest, supporting the argument of changing operational priorities or seasonal differences.

4.2.3 Changes in Stockpile Volume Based on Material Type

Stockpile volume changes based on the material types helps identify the commonly manufactured materials in the sites and their temporal volume change dynamics. For ease of assessment, materials have been grouped together into types in the Iron Making and Pellet Plant project as

presented in Table 10. Materials in the Steel Making project are not grouped. The known material properties are also presented in Table 10. Unknown material properties are marked as N/A.

Table 10: Material Properties

Project	Material Type	Grouped Sub-types	Density (tns/m³)	Moisture (%)
Iron Making	Coal	Alpine coal	0.86	0.11
		Bedford coal	0.86	0.11
		Bedford/ LV	0.86	0.11
		BHPA coal	0.86	0.11
		Blended coal	0.86	0.11
		Coal being built	0.86	0.11
		Coal being reclaimed	0.86	0.11
		Lake vermont coal	0.86	0.11
	Coke	Blast furnace nut returns	0.55	0.1
		Blast furnace nut returns imported	0.9	0.055
		Blast furnace coke	0.5	0.055
		Bluescope 2	0.5	0.052
		Coke	0.55	N/A
		Coke breeze	0.66	0.15
		Import coke	0.01	0.085
		Large coke	0.55	N/A
		Large nut coke	0.55	0.1
		Nisco 2	0.5	0.048
		Nisco 3	0.5	0.038
		Nisco coke	0.5	0.048
		Nut coke	0.55	0.1
		Nut returns	0.55	0.1
		Scalping coke	0.5	0.06
		Small nut coke	0.55	0.1
	Dolomite	Contaminated dolomite fines	N/A	N/A
		Dolomite aggregate	1.52	0.005
		Dolomite fines	1.53	0.035
		Dolomite lump	1.51	0.005
		Dolomite (Penrice)	1.46	0.005
	Limestone	Japanese limestone lump	1.46	0.005
		Limestone	1.55	0.03
		Limestone fines	1.46	0.005
		Limestone lump	1.46	0.005
		Limestone lump (Greymont)	1.46	0.005
		Limestone lump (Penrice)	1.46	0.005
	QBB	Quencher basin	0.55	0.15
		Quencher basin breeze	0.66	0.15
		Quencher basin product	0.55	0.15
	Quartz	Blast furnace quartz	1.49	N/A
	Slag	Slag	N/A	N/A
	Sulphate	Ammonium sulphate	1.05	N/A
	Centrix	Centrix	2.15	0.01
		Kiln ring	2.03	N/A

Project	Material Type	Grouped Sub-types	Density (tns/m³)	Moisture (%)
Pellet Plant	Manufactured raw materials	Filter cake	2.2	N/A
		Magnetite pellets	1.98	0.01
		Pellet chips	2.15	0.01
		Pellets	1.98	0.01
	Ores	Blast furnace lump	2.2	N/A
		Iron ore fines	N/A	N/A
		Iron ore lump	N/A	N/A
		Lump fines	N/A	N/A
		Lump ore	N/A	N/A
		Ore fines	N/A	N/A
Steel Making		Aldex briquettes	0.98	N/A
		Aluminium pucks	1.5	N/A
		Bauxite	1.3	N/A
		Contaminated Alloys	1.1	N/A
		Ferro manganese H.C.	3.95	N/A
		Ferro manganese M.C.	4	N/A
		Ferro silicon 75%	1.7	N/A
		HCFeCr	3.92	N/A
		Low Ali FeSi	1.7	N/A
		Quartz for LMF	1	N/A
		Silicon manganese	3.49	N/A

Based on the grouped material types presented in Table 10, the total sum of materials was computed for every month. This is presented in Table 11. Coke and Coal were found to be the most abundant material types in the Iron Making Project with a mean survey volume of 85746 m³ and 60026 m³ respectively. In addition, Coal had a higher value for CV 54% compared to Coke, 29% indicating a higher fluctuation of material volume per month.

Similarly in Pellet Plant, the manufactured raw materials contributed to a big portion of the monthly mean stockpile volume at 104998 m³ with a CV of only 18%. Centrix was the only other major contributor to volume with a mean of 39038 m³ and a CV of 11%. These numbers suggest minor fluctuations in the material volumes in this project. Overall, these two kinds of materials add up to 98.7% of the total stockpile volume in this project.

On the contrary, Steel Making records a much lower volume of stockpiles with the largest contributors being Ferro Manganese H.C. and Silicon Manganese at a mean volume of 781 m³ and 700 m³ and a CV of 17% and 24% respectively.

Table 11: A summary of the monthly volume based on material composition of all stockpiles.

MATERIAL	Jan	Feb	Mar	Apr	May	Jun	Jul	Aug	Sep	Oct	Nov	Dec	*Grand Total*
IRON MAKING	**292495**	**314440**	**312761**	**255788**	**266393**	**263773**	**231692**	**211272**	**241727**	**160820**	**95957**	**190879**	***2837997***
COAL	83988	103503	92697	63790	89754	89929	42592	70594	51062	7629	5092	19687	*720317*
COKE	119893	115116	99861	88778	61767	46900	97643	71101	103944	94907	44170	84872	*1028952*
DOLOMITE	30373	29710	28352	23450	40354	38233	33187	20502	37538	22103	18298	34817	*356917*
LIMESTONE	35586	34445	51254	42181	29187	42636	32849	26115	25559	18548	13019	35359	*386738*
MILLSCALE	900	1212	1877	2223	2837	2902	3228	3984	4446	4543	4750	4874	*37776*
QBB	12849	13357	12831	12467	14729	17585	20456	17483	17819	11811	9627	8873	*169887*
QUARTZ	1706	1572	1309	1203	1085	942	804	746	642	605	373	1187	*12174*
SLAG	4267	12233	19556	18442	23767	21778							*100043*
SULPHATE	926	720	856	541	584	772	578	391	370	296	270	224	*6528*
UNKNOWN	2007	2572	4168	2713	2329	2096	355	356	347	378	358	986	18665
PELLET PLANT	**143477**	**155811**	**182517**	**168035**	**146155**	**165796**	**150536**	**122875**	**122413**	**126939**	**118995**	**148095**	***1751644***
CENTRIX	40708	43172	41821	37966	38907	40874	41794	42111	42396	43602	27353	27754	468458
MANUFACTURED RAW MATERIALS	101099	111043	138669	127070	104594	122482	106707	78476	78044	81929	90592	119272	1259977
ORES	1553	1473	1899	2883	2542	2318	1910	2161	1850	1281	924	941	21735
UNKNOWN	117	123	128	116	112	122	125	127	123	127	126	128	1474
STEEL MAKING	**2846**	**3236**	**2634**	**2481**	**2113**	**2341**	**2773**	**2407**	**2544**	**2568**	**2335**	**2705**	***30983***
ALDEX BRIQUETTES	92	119											*211*
ALUMINIUM PUCKS	69	34	43	38	15	21	31	25	55	54	92	105	*582*
BAUXITE	217	185	384	258	224	166	240	147	63	16	23	272	*2195*
CONTAMINATED ALLOYS	159	157	157	156	158	156	159	158	157	156	158	158	*1573*
FERRO MANGANESE H.C.	631	915	824	743	650	587	1005	911	930	836	674	667	*9373*
FERRO MANGANESE M.C.	151	112		120	111	96	114	124	117	108	104	96	*1253*
FERRO SILICON 75%	257	288	195	319	254	315	344	308	279	308	331	435	*3633*
HCFeCr	73	62	55	37	50	46	37	37	33	28	51	51	*560*
LOW ALI FeSi			60	52	56		28	111	60	45	37	39	*488*
QUARTZ FOR LMF	161	166	130	84	108	139	105	111	133	135	186	188	*1646*
SILICON MANGANESE	457	1026	786	674	487	815	710	475	717	882	679	694	*8402*
UNKNOWN	579	172											*1067*
Grand Total	**438818**	**473487**	**497912**	**426304**	**414661**	**431910**	**385001**	**336554**	**366684**	**290327**	**217287**	**341679**	***4620624***

In order to identify the temporal trend of specific material volume changes, Figure 25, Figure 26 and Figure 27 present the changes in volume in a waterfall chart. The first bar represents the initial sum of volumes for each material type and each of the following bar represents the change from the

previous survey. The incremental/decremental change in volume is labelled as a percentage change from the prior survey.

Figure 25 depicts the volume changes in material types across the Iron Making Project. 8 of the 9 material types were surveyed throughout the year with Slag being the only exception. The first two months contained the peak survey volume for 5 of the 9 material types. A decreasing trend in volume can be observed in 7 of the 9 material types. The last two months of the year contain the lowest survey volume in 7 of the 9 material types with the November having the least value in 5 of them. There is a clear pattern of decreasing volume trend although 6 of the 8 sites that have been surveyed throughout the year have an increase in volume in December. Overall, there is a large fluctuation in volume over the year in every material type barring Millscale which is the only material type that serves as an outlier with consistent volume growth over the year.

Similarly, in Figure 26, changes in the Pellet Plant project can be observed. In 2 of the 3 material types surveyed, the lowest recorded volume is in November with a slight increase in December. Manufactured raw materials is slightly different with its trough occurring in September leading to slight increases till December. In all three material types, the crest can be observed in the first four months of the year. Manufactured raw materials and ores then consistently decline while Centrix volume has slight increases till October with a sharp fall in November. Centrix volumes remain close to 40000 m^3 for the first 10 months of the year with large variations in the other two material types. Largely, the patterns observed in Pellet Plant is very similar to that in Iron making of high volumes in initial months with gradual decline till the end of year.

Steel Making is slightly different compared to the other two projects with a much lower mean volume in all material types. Figure 27 shows the temporal volume changes in Steel Making material types with only 2 of the 9 materials exhibiting a trend similar to the Iron Making and Pellet Plant projects, i.e. high initial volume following a decline. 2 other discernible trends are observable: a decline till mid-year followed by an increase and an alternating pattern of increment and decrement.

Figure removed due to copyright restriction

Figure 25: Changes in monthly stockpile volume based on material type in Iron Making

Figure removed due to copyright restriction

Figure 26: Changes in monthly stockpile volume based on material type in Pellet Plant

Figure removed due to copyright restriction

Figure 27: Changes in monthly stockpile volume based on material type in Steel Making

4.3 Effect of Footprint Area and Perimeter on Volume Change

The relationship between footprint area and perimeter on volume is analysed using scatterplots. Figure 28 and Figure 29 plot stockpile perimeter and area respectively against volume to understand the growth in volume corresponding to increase in these variables. The power curve trendline makes the best fit to the data, especially at lower values of area and perimeter suggesting a non-linear relationship with accelerating volume increase with increase in footprint area. However, there is a noticeable dispersion from the trendline at higher values of these variables indicating these variables alone do not account for the volume changes. Table 12 presents the trendline equations for both

these variables. The R^2 value indicates that footprint area explains 76% of the volume changes which is a better predictor than toe line perimeter.

Table 12: Explanatory variable details

Explanatory Variable	R^2 Value	Trendline Equation
Perimeter	0.54	$y = 0.0048x^{2.5925}$
Area	0.76	$y = 0.1301x^{1.3836}$

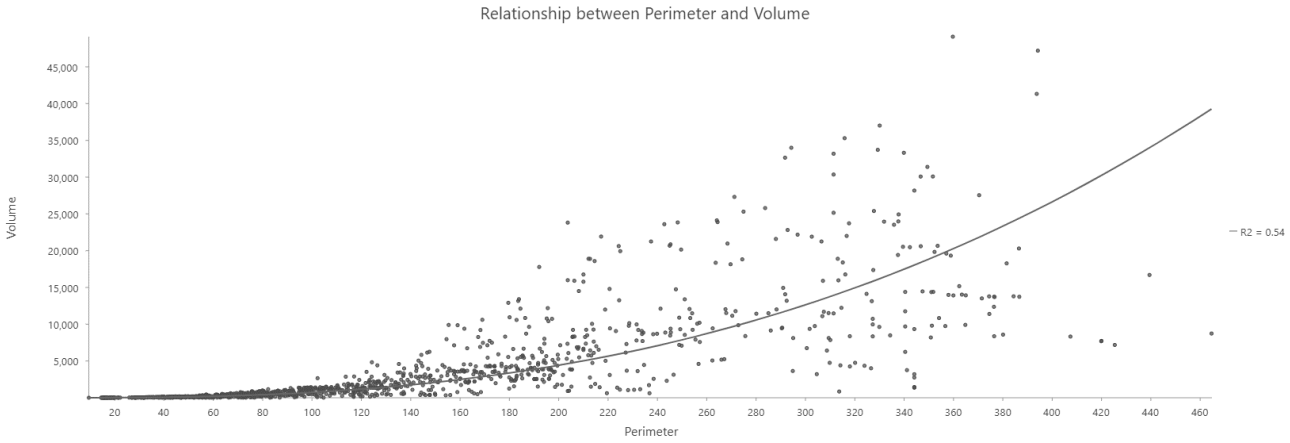

Figure 28: Scatterplot of stockpile perimeter vs volume.

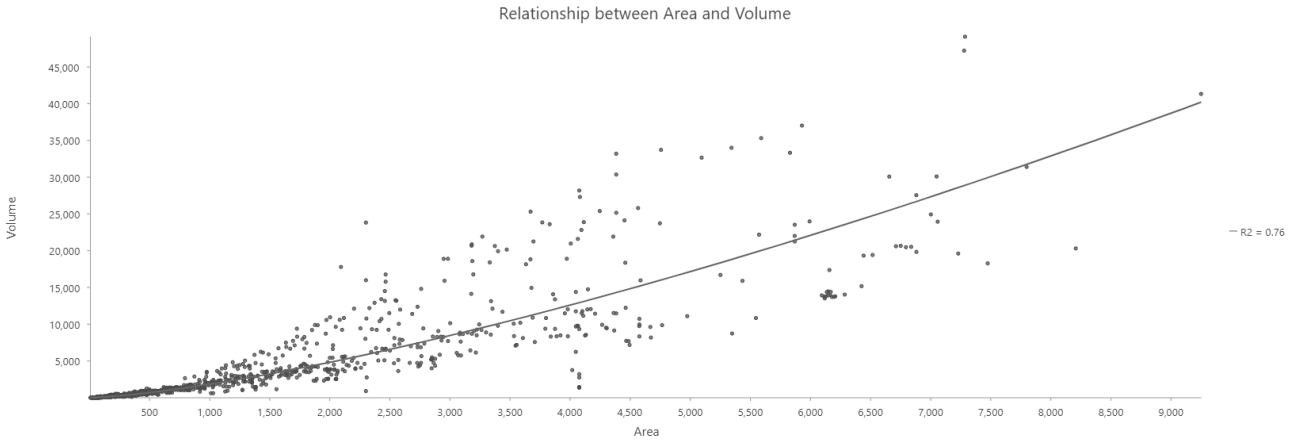

Figure 29: Scatterplot of stockpile area vs volume.

5 DISCUSSION

This study demonstrated a successful stockpile monitoring methodology using UAV photogrammetry, integrated data processing and advanced visualization techniques. This study has provided a workflow for enhancing the accuracy, efficiency, and accessibility of stockpile management processes. This workflow addresses challenges associated with stockpile management such as manual labour intensity, error susceptibility and inefficiencies in data processing and reporting.

The use of UAV photogrammetry for high-resolution aerial imagery capture combined with photogrammetry software such as Agisoft Metashape allowed for consistent data processing and the generation of detailed 3D models. The management of data through integrated geodatabase allowed for ease of access, storage and analysis. The ability to track changes and identify trends is particularly valuable for decision making. Furthermore, the implementation of cutting-edge reporting and visualization tools such as static tiered maps and web-based dynamic visualization can be utilized to facilitate a better understanding of stockpile dynamics and enhanced data communication.

With the well-established relationship between inventory management and operational efficiency as well as profit making, this study aimed to provide a robust stockpile monitoring methodology based on research into the most efficient volume computation techniques and data delivery platforms.

The workflow presented in this study is designed to meet the needs of stockpile management. However, the principles are applicable for implementation across a variety of industries. The scalability and adaptability of this workflow makes it a valuable tool for any number of applications. Additionally, with improvements in technology, stockpile management practices can be further enhanced to achieve higher accuracy and efficiency.

5.1 Stockpile Volume Computation and Monitoring Methodology

One of the main goals of the study was to establish a robust and efficient methodology for computing and monitoring stockpile volumes. The study began a review of existing workflow into stockpile volume calculation along with advanced methods of data delivery and communication. The resulting methodology included data collection, which included choosing the right camera, flying height, flight path and optimal image overlaps. For precise photogrammetric reconstruction, UAVs were set up to acquire high-resolution aerial imagery with substantial front and side overlap. GNSS was used to survey and position Ground Control Points (GCPs) ensuring high spatial accuracy and minimizing discrepancies during model building. Precise camera positioning was ensured using PPK/RTK approaches for error correction. This two-pronged strategy enabled a high degree of accuracy of the resultant model.

Photogrammetric data processing involved stages of aerial triangulation and bundle block adjustment for generation of tie points that were transformed from image space co-ordinate system to a geographic co-ordinate system. GCPs established during the data acquisition served to accurately georeferenced the model. Detailed 3D representation of stockpiles was created through the densification of the sparse point clouds. These dense point clouds were used for the volume computation process while orthophotos were generated for accurate planimetric representation of the surveyed sites.

The resultant densified point cloud from the photogrammetric process was meticulously cleaned before commencing the volume computation process. This entailed the removal of extraneous objects such as buildings, vehicles, vegetation and conveyors. The cleaned point clouds were turned into 3D TINs for volume calculation. In cases of absence of a pre-existing base model, toe lines were manually drawn around the stockpiles to delineate the approximate ground surface. Finally, the volume of the 3D stockpile TIN was calculated over the base 3D TIN. This process was repeated for every stockpile captured throughout the survey period.

5.2 Database and Visualization

The organization and management of large dataset resulting from the survey of a total of 1365 stockpiles over the study period necessitated the creation of a comprehensive database. The database structure was designed to integrate the survey metadata, stockpile material metadata and the computed stockpile volume and dimensions as presented in Table 5. This systematic approach guaranteed the accessibility of all pertinent data in a unified framework. Scripts (native to the javascript language) were developed to automate the tasks of stockpile volume and footprint extraction from 3DR, which streamlined the establishment and maintenance of the database. Layers of geographic data were managed using GIS improving the database's capacity to perform spatial analysis and visualization. Database accuracy was maintained by validating the data (ensuring footprint polygons contain valid geometries and line up with orthophotos) before updating the database. Random volume checks were done to further ensure data accuracy.

This study had a real-world application with monthly reports being submitted to the clients. The pre-existing reporting methodology (section 4.1.1) posed several limitations. Firstly, the use of manual data entry into tables introduces the risks of data entry errors and is cumbersome. Additionally, static tables and images also do not allow for data exploration and have limited visualization capabilities. Furthermore, data integration from multiple surveys presents a challenge when overlaying numerous datasets. Finally, any form of data revision is prone to inconsistency with no capabilities of maintaining versioning. During the course of this project, the reporting methods were transitioned from conventional spreadsheet-based reporting to a tiered map-based reporting. With the use of tiered maps: overview plans, location index plans, and stockpile volume plans; stockpile data could be visualised in great detail improving comprehension and dissemination of survey findings.

Furthermore, a web-based visualization platform is implemented to enhance the reporting and visualization of stockpile data. The web-based application would allow stakeholders to easily access and utilize stockpile data owing to the application's dynamic and interactive visualization capabilities served in a user-friendly manner. Interactive online maps equipped with pop-up windows that display summary information, dynamic charts, and tables that respond to user interactions and changes in the map extent were created to present stockpile data across several projects and time periods. This would enable real-time monitoring and assessment of stockpiles and serve as a unified and centralized repository of vital information which has potential to be used as a spatial and temporal analyses platform. Additionally, it would vastly improve the reporting and monitoring process making it incredibly engaging and informative.

The transition to modern methods of databasing and visualization as presented in this study is extremely beneficial in the field of stockpile management. Data accuracy and accessibility is significantly improved while simultaneously moving away from tedious and error-prone manual data entry and physical record keeping practices. With the power of web-GIS, real time data visualization and exploration is achieved. This is highly beneficial to any industry where information on inventory changes is critical to operational gains. The scalability of a digital database and web-based visualization is also substantial. The system can be expanded to accommodate additional data, locations and materials ensuring adaptability to changing requirements. Other applications such as soil and crop volume monitoring, landfill capacity monitoring, post-disaster debris volume monitoring can adapt this methodology for their needs. This highlights the customizability of the workflow for different purposes and integration into various industries aligning with the concepts from Gaspari et al. (2022).

5.3 Temporal and Spatial Analyses

In order to gain insights into stockpile change dynamics, several temporal and spatial analyses were conducted. Monthly survey data were examined for patterns and changes in the volume of stockpiles over time. The emerging patterns shed light on the operational priorities and seasonal fluctuations of stockpile volumes (Figure 22, Figure 23 and Figure 24). These also revealed sites that were hotspots for volume accumulation. Additionally, the stockpile volumes based on material types revealed patterns of material volume changes over time (Figure 25, Figure 26 and Figure 27).

5.4 Limitations of UAV Photogrammetry

Although UAV photogrammetry offers numerous benefits for stockpile management, several limitations can impact its accuracy, efficiency and feasibility. Understanding these limitations is vital for optimizing the use of UAVs in diverse environments and ensuring robust results.

The narrow battery life of UAVs directly impacts flight duration. In general, commercial UAVs battery life range from 20-40 minutes based on environmental conditions and the weight of the payload. This creates challenges for very large stockpiles or the survey of large areas with multiple flight obligations for complete coverage. Frequent battery changes and recharging can disrupt operations and extend the total survey time needed for data collection. In addition, changes in the lighting conditions during multiple flights can cause problems in photogrammetric data processing (Colomina & Molina, 2014).

Another challenge faced in stockpile surveys using UAVs is its operation in confined spaces such as indoor storage facilities or areas with dense infrastructure. This restricts manoeuvrability and increases risks of collisions. Additionally, UAVs are reliant on GPS signals for positioning so any loss of GPS signals in such environments is a hindrance to precise camera positioning leading to unreliable photogrammetric results (Siebert & Teizer, 2014).

UAV photogrammetry is also reliant on GNSS for the georeferencing of the model. This causes issues in areas with limited or no GNSS coverage such as urban canyons, dense forests or underground environments. The accuracy of UAV photogrammetry is compromised in these environments. The use of precise GCPs and integrated IMUs in modern UAVs help but don't fully mitigate the problem (Nex & Remondino, 2014).

UAV operations are also impacted by weather conditions. Adverse weather conditions such as strong winds, rain, fog or extreme temperatures affect the safety and stability of the UAV and compromises image quality causing issues such as motion blur, inadequate lighting and reduced image resolution. Ultimately, this reduces the accuracy and reliability of the resulting models (Hardin & Jensen, 2011).

The substantial computational requirements of photogrammetric data processing are also a limitation for users. The need for powerful and expensive hardware and software can be a big obstacle for widespread implementation. The processing time increases with detail and surveyed area causing delays in analysis.

5.5 Implication for Inventory Management

For inventory management to be effective, timely and accurate data on stockpile amounts are essential. The precise and regular data that UAV photogrammetry offers is required to enhance supply chain management, optimise resource allocation, and make responsible operational choices. Routine stockpile volume monitoring allows organizations to achieve the following:

Optimise Resource Allocation: Precise volume measurements provide improved resource planning and allocation, guaranteeing materials availability and mitigating the risk of overstocking or shortages. The accuracy of stockpile evaluations may be greatly increased by using UAV-based inventory identification and quantification (Tsakiridis & Papakonstantinou, 2024).

Boost Supply Chain Management: Accurate demand forecasting and more effective supply chain management are made possible by regular updates on stockpile amounts. As a result, there is an improvement in lead times, overall supply chain responsiveness, and collaboration between suppliers and consumers. It has been demonstrated that inventory management in industrial settings may be optimised by integrating UAVs with LiDAR technology (Tsakiridis & Papakonstantinou, 2024; Mahlberg et al., 2024).

Enhance Decision-Making: Managers may decide on production plans, inventory levels, and procurement strategies with knowledge of detailed stockpile dynamics. Better financial performance and more efficient operations are the results of this data-driven strategy. According to studies (Adjidjonu & Burgett, 2019; Brezani et al., 2021), UAV photogrammetry can deliver precise and dependable data for decision-making processes.

Analysis: Trend analysis and performance evaluation are further supported by the capacity to monitor stockpile changes over time. Organisations may create more effective inventory management strategies and boost overall operational efficiency by knowing how stockpile amounts vary seasonally or in response to operational changes. Studies have indicated how UAV photogrammetry may be used to monitor these changes and improve resource allocation (Pavelka et al., 2023; Whitehead et al., 2014).

6 CONCLUSIONS AND RECOMMENDATIONS

6.1 Conclusions

The study aimed to enhance stockpile volume computation and reporting with the application of UAV photogrammetry. This resulted in a demonstration of a robust methodology for stockpile monitoring with the creation of a comprehensive stockpile database, enhanced reporting and visualization techniques and conducted spatial and temporal analysis of the change in stockpile volume throughout the study period. The findings provide insights into the application and benefits of UAV photogrammetry in stockpile management.

The collection of high-resolution data in complicated locations with minimal human intervention using UAVs has proven to increase operational efficiency. These methods significantly outperform the conventional techniques of stockpile volume computation aligning with the study by Ajayi and Ajulo (2021) who emphasized the capability of UAVs to reduce manual labour and minimize safety hazards without compromising accuracy.

The unique approach in this study is the implementation of databasing and modern visualization to supplement the UAV based workflow in stockpile monitoring. Several studies have demonstrated the successful implementation of UAVs in volume computation and monitoring. In addition to that, the utilization of spatial databases, GIS and visualization platform enhances data delivery and communication vital to planning and informed decision making. The development of a detailed stockpile database facilitated inventory management and planning. With key survey and material attributes incorporated alongside the essential spatial and volume information within a database, the database offered a strong foundation for analyses. Raeva et al. (2016) who highlighted the need of precise data for accurate volume estimation and resource allocation. In the case of this study, precise data alongside pertinent information integrated in a database allows for granular analysis. The insights into stockpile dynamics, material utilisation, and inventory trends that could be obtained by temporal and spatial analyses supported the conclusions of Gaspari et al. (2022) about the significance of understanding changes in stockpile volume over time.

The notable improvements in data accessibility and communication resulting from the transition from conventional spreadsheet-based reporting to a dynamic web-based visualization reinforced the advantages of real-time data exploration as mentioned by Ai et al. (2015) and Adjidjonu and Burgett (2019). This transition improved the overall communication of stockpile information leading to a highly efficient stockpile management system. As reported by Mora et al. (2020), these findings highlight the gains in operating efficiency with the use of UAV photogrammetry's capability of providing rapid data acquisition, high-resolution imagery and the ability to operate in diverse and challenging environments.

As a result, this study demonstrates that UAV photogrammetry is a feasible and beneficial approach for the computation and monitoring of stockpiles. The integration of advanced technology and innovative approaches has resulted in substantial enhancements in precision, safety, and efficiency. The findings of this research contribute to the expanding evidence supporting the use of UAV photogrammetry for stockpile management as well as other similar domains, highlighting its potential to revolutionize traditional methods and offer significant operational advantages.

6.2 Recommendations

The following recommendations are made in order to further enhance the use of UAV photogrammetry in stockpile management and similar other fields.

First and foremost, the application of UAV photogrammetry in stockpile management sectors should become a standard practice as it has several advantages compared to traditional methods as emphasized by this study and others (Ajayi & Ajulo, 2021; Alsayed et al., 2021). The integration of LiDAR technology with UAV photogrammetry could prove to be fruitful in providing higher accuracy and mitigate the challenges of monitoring stockpiles under vegetation as shown by Gaspari et al. (2022). The precision of the generated models can be improved using well-distributed GCPs and the incorporation of quality check points.

To further improve on this study, the stockpile database can be augmented with more features. A relational database system would significantly boost the capabilities of the current database. It would increase the efficiency of querying and analysis and enable better integration with other systems. The web-based application developed in this project has demonstrated significant advances in reporting and data visualization. This could be further enhanced by integrating options for communicating flight planning parameters into the application such that all relevant project information would be housed in a single repository. This would certainly increase the overall effectiveness of stockpile management operations, streamline the process and reduce the potential for errors.

Furthermore, the addition of 3D visualization capabilities to the application can aid in a detailed inspection of the stockpiles. This could help the stakeholders analyse the shape of the stockpiles and increase reporting transparency. It is also crucial to educate the end-users about the capabilities of such a platform enabling them to access and analyse information proficiently. Moreover, a dynamic web-based tiled image delivery service can be utilized to depict the temporal changes of stockpile storage locations by showcasing the changing orthophotos of the stockpile storage locations.

In addition to volume computation of high value inventory commodities, this method also has advantages in the estimation of growing stock volume (GSV) which is critical to forest inventory

updating, terrestrial carbon stocks reporting and ecosystem services assessment. Chrysafis et al (2019) used Sentinel 1 imagery for stock volume estimation in Mediterranean forests with combination of spectral indices and texture models.

BIBLIOGRAPHY

Ai, M., Hu, Q., Li, J., Wang, M., Yuan, H., & Wang, S. (2015). A robust photogrammetric processing method of low-altitude UAV images. Remote Sensing (Basel, Switzerland), 7(3), 2302–2333. https://doi.org/10.3390/rs70302302

Adjidjonu, D. and Burgett, J. (2019). Optimal UAS Parameters for Aerial Mapping and Modeling. Available at: http://ascpro0.ascweb.org/archives/cd/2019/paper/CPRT255002019.pdf

Ajayi, O. G., & Ajulo, J. (2021). Investigating the Applicability of Unmanned Aerial Vehicles (UAV) Photogrammetry for the Estimation of the Volume of Stockpiles. Quaestiones Geographicae, 40(1), 25–38. https://doi.org/10.2478/quageo-2021-0002

Alsayed, A., & Nabawy, M. R. A. (2023). Stockpile Volume Estimation in Open and Confined Environments: A Review. Drones (Basel), 7(8), 537-. https://doi.org/10.3390/drones7080537

Alsayed, A., Yunusa-Kaltungo, A., Quinn, M. K., Arvin, F., & Nabawy, M. R. A. (2021). Drone-assisted confined space inspection and stockpile volume estimation. Remote Sensing (Basel, Switzerland), 13(17), 3356-. https://doi.org/10.3390/rs13173356

Arango, C., & Morales, C. A. (2015). Comparison between multicopter UAV and total station for estimating stockpile volumes. International Archives of the Photogrammetry, Remote Sensing and Spatial Information Sciences – ISPRS Archives, 40(1), 131–135. https://doi.org/10.5194/isprsarchives-XL-1-W4-131-2015

Awasthi, B., Karki, S., Regmi, P., Dhami, D., Thapa, S., & Panday, U. (2019). Analysing the Effect of Distribution Pattern and Number of GCPs on Overall Accuracy of UAV Photogrammetric Results. https://doi.org/10.1007/978-3-030-37393-1_29

Brezani, S., Hrasko, R., Vanco, D. and Vojtás, P. (2021). Increasing Business Opportunities for Drone Services. Available at: https://www.globesy.sk/wp-content/uploads/2023/02/1.-Increasing-Business-Opportunities-for-Drone-Services-GLOBESY-2021.pdf

Brown, N., Kaloustian, S., & Roeckle, M. (2007). Monitoring of Open Pit Mines Using Combined GNSS Satellite Receivers and Robotic Total Stations. Slope Stability 2007: Proceedings of the 2007 International Symposium on Rock Slope Stability in Open Pit Mining and Civil Engineering, Australian Centre for Geomechanics, Perth.

Chambers, D. W. (1989). Estimating Pit Excavation Volume Using Unequal Intervals. Journal of Surveying Engineering, 115(4), 390–401. doi:10.1061/(asce)0733-9453(1989)115:4(390)

Chen, S. et al. (2017) Measuring Vegetation Height in Linear Disturbances in the Boreal Forest with UAV Photogrammetry. Remote sensing (Basel, Switzerland). [Online] 9 (12), 1257-.

Chrysafis, I., Mallinis, G., Tsakiri, M., & Patias, P. (2019). Evaluation of single-date and multi-seasonal spatial and spectral information of Sentinel-2 imagery to assess growing stock volume of a Mediterranean forest. International Journal of Applied Earth Observation and Geoinformation, 77, 1–14. https://doi.org/10.1016/j.jag.2018.12.004

Colomina, I., & Molina, P. (2014). Unmanned aerial systems for photogrammetry and remote sensing: A review. ISPRS Journal of Photogrammetry and Remote Sensing, 92, 79–97. https://doi.org/10.1016/j.isprsjprs.2014.02.013

Connolly, T., & Begg, C. (2014). Database systems: a practical approach to design, implementation and management (Sixth edition, global edition.). Pearson Education.

Cryderman, C., Mah, S. B., & Shufletoski, A. (2014). Evaluation of UAV photogrammetric accuracy for mapping and earthworks computations. Geomatica (Ottawa), 68(4), 309–317. https://doi.org/10.5623/cig2014-405

Dai, H., & Jiying, J. (2022). Application of UAV Photogrammetry on Ecological Restoration of Abandoned Open-pit mines, Northern Anhui Province, China. Nature Environment and Pollution Technology, 21(1), 193–199. https://doi.org/10.46488/NEPT.2022.v21i01.021

Ekaso, D., Nex, F., & Kerle, N. (2020). Accuracy assessment of real-time kinematics (RTK) measurements on unmanned aerial vehicles (UAV) for direct geo-referencing. Geo-Spatial Information Science, 23(2), 165–181. https://doi.org/10.1080/10095020.2019.1710437

Elmasri, R., & Navathe, S. (2011). Fundamentals of database systems (6th ed.). Addison-Wesley.

Famiglietti, N. A., Cecere, G., Grasso, C., Memmolo, A., & Vicari, A. (2021). A test on the potential of a low cost unmanned aerial vehicle rtk/ppk solution for precision positioning. Sensors (Basel, Switzerland), 21(11), 3882-. https://doi.org/10.3390/s21113882

Ferrer-González, E., Agüera-Vega, F., Carvajal-Ramírez, F., & Martínez-Carricondo, P. (2020). UAV Photogrammetry Accuracy Assessment for Corridor Mapping Based on the Number and Distribution of Ground Control Points. Remote. Sens., 12, pp. 2447. https://doi.org/10.3390/rs12152447

Gaspari, F., Ioli, F., Barbieri, F., Belcore, E., & Pinto, L. (2022). Integration of UAV-LiDAR and UAV-photogrammetry for infrastructure monitoring and bridge assessment. The International Archives of the Photogrammetry, Remote Sensing and Spatial Information Sciences. https://doi.org/10.5194/isprs-archives-xliii-b2-2022-995-2022.

Giannetti, F., Chirici, G., Gobakken, T., Næsset, E., Travaglini, D., & Puliti, S. (2018). A new approach with DTM-independent metrics for forest growing stock prediction using UAV photogrammetric data. Remote Sensing of Environment, 213, 195–205. https://doi.org/10.1016/j.rse.2018.05.016

Gregory, S., Singh, U., Gray, J., & Hobbs, J. (2021). A computer vision pipeline for automatic large-scale inventory tracking. Proceedings of the 2021 ACM Southeast Conference. https://doi.org/10.1145/3409334.3452063.

Halim, A., Rahman, A., Maulud, K., Nekmat, M., & Mukhlisin, M. (2023). Assessment of Difference in Structure from Motion for Stockpile Volume Estimation using UAV Approach. IOP Conference Series: Earth and Environmental Science, 1240. https://doi.org/10.1088/1755-1315/1240/1/012002.

Hardin, P. J., & Jensen, R. R. (2011). Small-Scale Unmanned Aerial Vehicles in Environmental Remote Sensing: Challenges and Opportunities. GIScience and Remote Sensing, 48(1), 99–111. https://doi.org/10.2747/1548-1603.48.1.99

He, F., Zhou, T., Xiong, W., Hasheminnasab, S. M., & Habib, A. (2018). Automated aerial triangulation for UAV-based mapping. Remote Sensing (Basel, Switzerland), 10(12), 1952-. https://doi.org/10.3390/rs10121952

He, H., Chen, T., Zeng, H., & Huang, S. (2019). Ground control point-free unmanned aerial vehicle-based photogrammetry for volume estimation of stockpiles carried on barges. Sensors (Basel, Switzerland), 19(16), 3534-. https://doi.org/10.3390/s19163534

Hoffer, J., Venkataraman, R., Topi, H., & Hoffer, J. (2019). Modern Database Management, Global Edition (13th ed.). Pearson Education, Limited.

Hugenholtz, C., Walker, J., Brown, O., & Myshak, S. (2015). Earthwork Volumetrics with an Unmanned Aerial Vehicle and Softcopy Photogrammetry. Journal of Surveying Engineering-asce, 141, 06014003. https://doi.org/10.1061/(ASCE)SU.1943-5428.0000138.

James, M. R., Robson, S., & Smith, M. W. (2017). 3-D uncertainty-based topographic change detection with structure-from-motion photogrammetry: precision maps for ground control and directly georeferenced surveys. Earth Surface Processes and Landforms, 42(12), 1769–1788. https://doi.org/10.1002/esp.4125

Jiménez-Jiménez, S. I., Ojeda-Bustamante, W., Marcial-Pablo, M. D. J., & Enciso, J. (2021). Digital terrain models generated with low-cost UAV photogrammetry: Methodology and accuracy. ISPRS International Journal of Geo-Information, 10(5), 285-. https://doi.org/10.3390/ijgi10050285

Khanal, M., Hasan, M., Sterbentz, N., Johnson, R., & Weatherly, J. (2020). Accuracy Comparison of Aerial Lidar, Mobile-Terrestrial Lidar, and UAV Photogrammetric Capture Data Elevations over Different Terrain Types. Infrastructures. https://doi.org/10.3390/infrastructures5080065.

Kirk, A. (2016). Data visualisation: A handbook for data driven design. SAGE.

Kim, Y. H., Shin, S. S., Lee, H. K., & Park, E. S. (2022). Field Applicability of Earthwork Volume Calculations Using Unmanned Aerial Vehicle. Sustainability (Basel, Switzerland), 14(15), 9331-. https://doi.org/10.3390/su14159331

Kroenke, D. M., & Auer, D. J. (2015). Database concepts (Seventh edition, Global edition.). Pearson Education Limited.

Lau, L., & Tai, K. W. (2023). A Data Quality Assessment Approach for High-Precision GNSS Continuously Operating Reference Stations (CORS) with Case Studies in Hong Kong and Canada/USA. Remote Sensing (Basel, Switzerland), 15(7), 1925-. https://doi.org/10.3390/rs15071925

Lee, K., & Lee, W. H. (2022). Earthwork Volume Calculation, 3D Model Generation, and Comparative Evaluation Using Vertical and High-Oblique Images Acquired by Unmanned Aerial Vehicles. Aerospace, 9(10), 606-. https://doi.org/10.3390/aerospace9100606

Linder, W. (2003). Digital Photogrammetry Theory and Applications (1st ed. 2003.). Springer Berlin Heidelberg. https://doi.org/10.1007/978-3-662-06725-3

Liu, J., Hasheminasab, S. M., Zhou, T., Manish, R., & Habib, A. (2023). An Image-Aided Sparse Point Cloud Registration Strategy for Managing Stockpiles in Dome Storage Facilities. Remote Sensing (Basel, Switzerland), 15(2), 504-. https://doi.org/10.3390/rs15020504

Lemmens, M. (2016). Total stations: The surveyor's workhorse. GIM International, 30(10), 20–25.

Luhmann, T. (2013). Close-Range Photogrammetry and 3D Imaging (2nd ed.). De Gruyter. https://doi.org/10.1515/9783110302783

Mahajan, G., (2021). Applications of Drone Technology in Construction Industry: A Study 2012-2021. Available at: https://www.researchgate.net/profile/Argayatri-Mahajan-2/publication/355780706_Applications_of_Drone_Technology_in_Construction_Industry_A_Study_2012-2021/links/620a086b87866404a1685d24/Applications-of-Drone-Technology-in-Construction-Industry-A-Study-2012-2021.pdf

Mahlberg, J.A., Malackowski, H., Joseph, M. and Koshan, Y. (2024). Statewide Implementation of Salt Stockpile Inventory Using LiDAR Measurements: Case Study. Remote Sensing, 16(2). Available at: https://www.mdpi.com/2072-4292/16/2/410/pdf

Mahlberg, J.A., Manish, R., Koshan, Y., Joseph, M. and Liu, J. (2022). Salt stockpile inventory management using LiDAR volumetric measurements. Remote Sensing, 14(19). Available at: https://www.mdpi.com/2072-4292/14/19/4802/pdf

Manish, R., Hasheminasab, S. M., Liu, J., Koshan, Y., Mahlberg, J. A., Lin, Y.-C., Ravi, R., Zhou, T., McGuffey, J., Wells, T., Bullock, D., & Habib, A. (2022). Image-Aided LiDAR Mapping Platform and Data Processing Strategy for Stockpile Volume Estimation. Remote Sensing (Basel, Switzerland), 14(1), 231-. https://doi.org/10.3390/rs14010231

Mantey, S., & Aduah, M. (2021). Comparative Analysis of Stockpile Volume Estimation using UAV and GPS Techniques. https://doi.org/10.4314/gm.v21i1.1

Mlambo, R., Woodhouse, I., & Anderson, K. (2017). Structure from Motion (SfM) Photogrammetry with Drone Data: A Low Cost Method for Monitoring Greenhouse Gas Emissions from Forests in Developing Countries. Forests, 8, 68. https://doi.org/10.3390/F8030068.

Mora, O. E., Chen, J., Stoiber, P., Koppanyi, Z., Pluta, D., Josenhans, R., & Okubo, M. (2020). Accuracy of stockpile estimates using low-cost sUAS photogrammetry. International Journal of Remote Sensing, 41(12), 4512–4529. https://doi.org/10.1080/01431161.2020.1723167

Nex, F., & Remondino, F. (2014). UAV for 3D mapping applications: a review. Applied Geomatics, 6(1), 1–15. https://doi.org/10.1007/s12518-013-0120-x

Pavelka, K., Matoušková, E. and Pavelka Jr, K., (2023). Remarks on Geomatics Measurement Methods Focused on Forestry Inventory. Sensors, 23(17). Available at: https://www.mdpi.com/1424-8220/23/17/7376

Puliti, S., Breidenbach, J., & Astrup, R. (2020). Estimation of forest growing stock volume with UAV laser scanning data: Can it be done without field data? Remote Sensing (Basel, Switzerland), 12(8), 1245-. https://doi.org/10.3390/RS12081245

Raeva, P. L., Filipova, S. L., & Filipov, D. G. (2016). Volume computation of a stockpile – A study case comparing GPS and UAV measurements in an open pit quarry. International Archives of the Photogrammetry, Remote Sensing and Spatial Information Sciences., XLI-B1, 999–1004. https://doi.org/10.5194/isprs-archives-XLI-B1-999-2016

Sanz-Ablanedo, E., Chandler, J., Rodríguez-Pérez, J., & Ordóñez, C. (2018). Accuracy of Unmanned Aerial Vehicle (UAV) and SfM Photogrammetry Survey as a Function of the Number and

Location of Ground Control Points Used. Remote. Sens., 10, 1606. https://doi.org/10.3390/RS10101606

Schenk, T. (1997). Towards automatic aerial triangulation. ISPRS Journal of Photogrammetry and Remote Sensing, 52(3), 110–121. https://doi.org/10.1016/S0924-2716(97)00007-5

Shao, M., & Yang, X. (2016). Experiment Development of Control Point Positioning Based on RTK, 179-182. https://doi.org/10.2991/ICAMCS-16.2016.36.

Shaw, L., Helmholz, P., Belton, D., & Addy, N. (2019). COMPARISON OF UAV LIDAR AND IMAGERY FOR BEACH MONITORING. The International Archives of the Photogrammetry, Remote Sensing and Spatial Information Sciences. https://doi.org/10.5194/ISPRS-ARCHIVES-XLII-2-W13-589-2019.

Siebert, S., & Teizer, J. (2014). Mobile 3D mapping for surveying earthwork projects using an Unmanned Aerial Vehicle (UAV) system. Automation in Construction, 41, 1–14. https://doi.org/10.1016/j.autcon.2014.01.004

Son, S. W., Kim, D. W., Sung, W. G., & Yu, J. J. (2020). Integrating UAV and TLS approaches for environmental management: A case study of a waste stockpile area. Remote Sensing (Basel, Switzerland), 12(10), 1615-. https://doi.org/10.3390/rs12101615

Tersine, R., & Toelle, R. (1984). Optimum stock levels for excess inventory items. Journal of Operations Management, 4, 245-258. https://doi.org/10.1016/0272-6963(84)90014-7.

Tsakiridis, S. and Papakonstantinou, A. (2024). Optimizing UAV-Based Inventory Detection and Quantification in Industrial Warehouses: A LiDAR-Driven Approach. WSEAS Transactions on Systems. Available at: https://wseas.com/journals/systems/2024/a285102-011(2024).pdf

Tucci, G., Gebbia, A., Conti, A., Fiorini, L., & Lubello, C. (2019). Monitoring and computation of the volumes of stockpiles of bulk material by means of UAV photogrammetric surveying. Remote Sensing (Basel, Switzerland), 11(12), 1471-. https://doi.org/10.3390/rs11121471

Tufte, E. R. (2001). The visual display of quantitative information (2nd ed.). Graphics Press.

Twigg, D. R. (1995). VOLUME COMPUTATIONS USING SHAPE FUNCTIONS. Survey Review, 33(255), 2–16. doi:10.1179/sre.1995.33.255.2.

Whitehead, K., Hugenholtz, C.H. and Myshak, S., (2014). Remote Sensing of the Environment with Small Unmanned Aircraft Systems (UASs), Part 2: Scientific and Commercial Applications. Journal of Unmanned Vehicle Systems, 2(2). Available at: https://cdnsciencepub.com/doi/pdf/10.1139/juvs-2014-0007

Wolf, P. R., Dewitt, B. A., & Wilkinson, B. E. (2014). Elements of Photogrammetry with Application in GIS (Fourth edition.). McGraw-Hill Education.

Wu, C., Yuan, Y., Tang, Y., & Tian, B. (2022). Application of Terrestrial Laser Scanning (TLS) in the Architecture, Engineering and Construction (AEC) Industry. Sensors, 22(1), 265. https://doi.org/10.3390/s22010265

Yao, J. (2017). Terrestrial Laser Scanning Intensity Correction by Piecewise Fitting and Overlap-Driven Adjustment. Remote Sensing, 9(11), 1090. https://doi.org/10.3390/rs9111090

I acknowledge the use of OpenAI in aiding in the planning, editing, and proofreading of my thesis. OpenAI. (2024). ChatGPT (June 24 version) [Large language model]. https://chat.openai.com/chat

I also acknowledge the use of Quillbot AI in simplifying the convoluted language found in academic texts for comprehension. QuillBot. (2024). QuillBot (June 2024 version). Retrieved from https://www.quillbot.com.

APPENDICES

Appendix A: Scripts used in methodology

Script name: extract polyline.js

Description: This script extracts boundary polylines of stockpiles in .dxf format that are used to create 3D TINs from point clouds in 3DR.

```
function ErrorMessage(iMessage) {
    var myDlg = SDialog.New("Error Message");
    myDlg.AddLine(iMessage, false, {}, 1);
    myDlg.Execute();
    throw new Error(iMessage);
}

function openMyproject(iName) {
    var isOpen = OpenDoc(iName, true, true).ErrorCode; // 3DR document is cleared and the defined 3DR project is opened
    if (isOpen == 1) {
        ErrorMessage("An error occurred. Impossible to open the 3DR file."); // print an error message if no success
    }
    else {
        print("Your project " + iName + " has been opened."); // throw a message to inform the opening of the file
    }
}
```

```
var fileNames = GetOpenFileNames("Select the file to open", "3DR files (*.3dr)", "D://");

var outputPath = new String();

outputPath = GetOpenFolder("Save Output as:", "K:/Scripts/Testing/Cyclone 3DR/Scripts-master/Custom");

if (outputPath == null) {

    outputPath = "K:/Scripts/Testing/Cyclone 3DR/Scripts-master/Custom";

}


var allMultilineCollection = [];

print(fileNames);

for (var count = 0; count < fileNames.length; count++) {

    openMyproject(fileNames[count]);

    var myMultilineCollection = SMultiline.All(2);

    var outMultilineCollection = [];

    for (var multiLineCount=0; multiLineCount < myMultilineCollection.length; multiLineCount++){

        var myMultiline = myMultilineCollection[multiLineCount];

        var multilineName = myMultiline.GetName();

        if (multilineName.endsWith("Contour")){

            print("Executing "+multilineName+"\n");

            outMultilineCollection.push(myMultiline);

            allMultilineCollection.push(myMultiline);

        }

    }
```

```
    var outputName = outputPath+(fileNames[count].substring(fileNames[count].lastIndexOf('\\') +
1)).replace(".3dr",".dxf");

    print("Creating "+ outputName);

    SSurveyingFormat.ExportProject(outputName,outMultilineCollection);

    ClearDoc();

}
```

Script Name: stockpile volume to csv.js

Description: This script extracts the volumes of stockpiles and their IDs in csv format from 3DR.

```
function ErrorMessage(iMessage) {

    var myDlg = SDialog.New("Error Message");

    myDlg.AddLine(iMessage, false, {}, 1);

    myDlg.Execute();


    throw new Error(iMessage);

}


function openMyproject(iName) {

    var isOpen = OpenDoc(iName, true, true).ErrorCode; // 3DR document is cleared and the
defined 3DR project is opened


    if (isOpen == 1) {

        ErrorMessage("An error occurred. Impossible to open the 3DR file."); // print an error
message if no success
```

```
    }
    else {
        print("Your project " + iName + " has been opened."); // throw a message to inform the opening of the file
    }
}

function SaveData(
    fileName // the file path
    , content // the content to write in the file
) {
    var file = SFile.New(fileName);
    // save the data
    if (!file.Open(SFile.WriteOnly))
        throw new Error('Failed to write file:' + fileName); // test if we can open the file

    // write the smultiline in the file
    file.Write(content);
    // Close the file
    file.Close();
}

var fileNames = GetOpenFileNames("Select the file to open", "3DR files (*.3dr)", "D://");
```

```
//write header

var csv = new String();

csv = "File,Stockpile ID,Cut Volume\n";


var outputPath = new String();

outputPath = GetSaveFileName("Save Output as:", "csv files (*.csv)", "D:/Scripts/Cyclone 3DR/Scripts-master/Custom/Utsav/stockpilevolumes.csv");

if (outputPath == null) {

    outputPath = "D:/Scripts/Cyclone 3DR/Scripts-master/Custom/Utsav/stockpilevolumes.csv";

}


for (var count = 0; count < fileNames.length; count++) {

    openMyproject(fileNames[count]);

    //getting all the labels in the document

    var label = SLabel.All(2);

    for (var i = 0; i < label.length; i++) {

        var a = label[i].GetFolderName();

        var res = label[i].GetCol(0);

        var b = res.ValueTbl[0];

        print("Stockpile ID: " + a + " Volume: " + Math.round(b));

        csv += fileNames[count] + "," + a + "," + Math.round(b) + "\n";

    }

}

ClearDoc();
```

```
//create the csv report

SaveData(outputPath, csv);
```

Script Name: waterfall_generator.py

Description: This script creates waterfall charts (Figure 25, Figure 26 and Figure 27) from monthly stockpile volume data.

```
import pandas as pd

import matplotlib.pyplot as plt

import numpy as np

from matplotlib.patches import Patch



def waterfall_chart(ax, df, title):

    # Initialize the start and end points

    df['Start'] = 0

    df['End'] = df['Value'][0]


    # Calculate start and end points and bar colors

    for i in range(1, len(df)):

        previous_value = df.loc[i-1, 'Value']

        current_value = df.loc[i, 'Value']

        if current_value >= previous_value:

            df.loc[i, 'Start'] = previous_value

            df.loc[i, 'End'] = current_value
```

```
            df.loc[i, 'Color'] = '#156082'
        else:
            df.loc[i, 'Start'] = current_value
            df.loc[i, 'End'] = previous_value
            df.loc[i, 'Color'] = '#e97132'

    # Ensure the first bar is colored correctly
    df.loc[0, 'Color'] = '#403e39'

    # Plot bars
    for i, row in df.iterrows():
        ax.bar(row['Month'], height=row['End'] - row['Start'], bottom=row['Start'], color=row['Color'],
edgecolor=row['Color'])

    # Adding percentage labels
    offset = df['Value'].max() / 100
    for i, row in df.iterrows():
        va = 'bottom'
        if i == 0:
            # For the first bar, use the data value as the label
            label_y = row['End'] + offset
            ax.text(i, label_y, f'{row["Value"]}', ha='center', va=va, fontsize=12, color=row['Color'],
fontstyle='oblique', fontweight='bold')
        else:
```

```
        if row['Color'] == '#156082':
            label_y = row['End'] + offset
        else:
            label_y = row['Start'] - offset
            va = 'top'
        if row["Percentage Change"] == -100.0:
            label_y = row['End'] + offset
            va = 'bottom'
        if row["Percentage Change"] != 0.0:
            ax.text(i, label_y, f'{row["Percentage Change"]:.0f}%', ha='center', va=va, fontsize=12,
color=row['Color'], fontstyle='oblique', fontweight='bold')


    # Adding horizontal guidelines
    y_min = 0
    y_max = df['Value'].max() * 1.1  # Adjust multiplier as needed
    ax.set_ylim(y_min,y_max)
    y_values = ax.get_yticks()
    for y in y_values:
        ax.hlines(y, xmin=-0.5, xmax=len(df)-0.5, colors='gray', linestyles='dashed', linewidth=1)


    # Plot configuration
    ax.set_title(title, fontsize=15, fontstyle='oblique', fontweight='bold')
    # ax.set_xlabel('Month', fontsize=10, fontstyle='oblique', fontweight='bold')
    ax.set_ylabel('Total Volume (m³)', fontsize=10, fontstyle='oblique', fontweight='bold')
```

```
    ax.tick_params(axis='x')
    # ax.tick_params(axis='x', rotation=45)

# Data for multiple material types in the format:
# ‘material1’:[Jan Value, Feb Value,…, Dec Value],
# ‘material2’:[Jan Value, Feb Value,…, Dec Value]

materials_data = {

}

# Create a 3x3 grid of subplots
fig, axs = plt.subplots(3, 3, figsize=(20, 20))
fig.tight_layout(pad=5)

# Populate each subplot with a waterfall chart
for ax, (material, values) in zip(axs.flatten(), materials_data.items()):
    data = {
        # 'Month': ['Jan 2023', 'Feb 2023', 'Mar 2023', 'Apr 2023', 'May 2023', 'Jun 2023',
        #           'Jul 2023', 'Aug 2023', 'Sep 2023', 'Oct 2023', 'Nov 2023', 'Dec 2023'],
        'Month': ['Jan', 'Feb', 'Mar', 'Apr', 'May', 'Jun',
                  'Jul', 'Aug', 'Sep', 'Oct', 'Nov', 'Dec'],
        'Value': values
    }
```

```
    df = pd.DataFrame(data)
    df['Change'] = df['Value'].diff().fillna(df['Value'])
    df['Percentage Change'] = df['Value'].pct_change().fillna(0) * 100

    waterfall_chart(ax, df, material)

# Create legend
legend_elements = [
    Patch(facecolor='#403e39', label='Initial Survey Volume'),
    Patch(facecolor='#156082', label='Increment in Volume'),
    Patch(facecolor='#e97132', label='Decrement in Volume')
]
plt.legend(handles=legend_elements, loc='upper center', fontsize=15, bbox_to_anchor=(-0.7, -0.07), fancybox=True, shadow=True, ncol=3)
plt.show()
```

Appendix B: Combined Orthophotos

Figure 30: Combined Orthophoto of all sites for January 2023

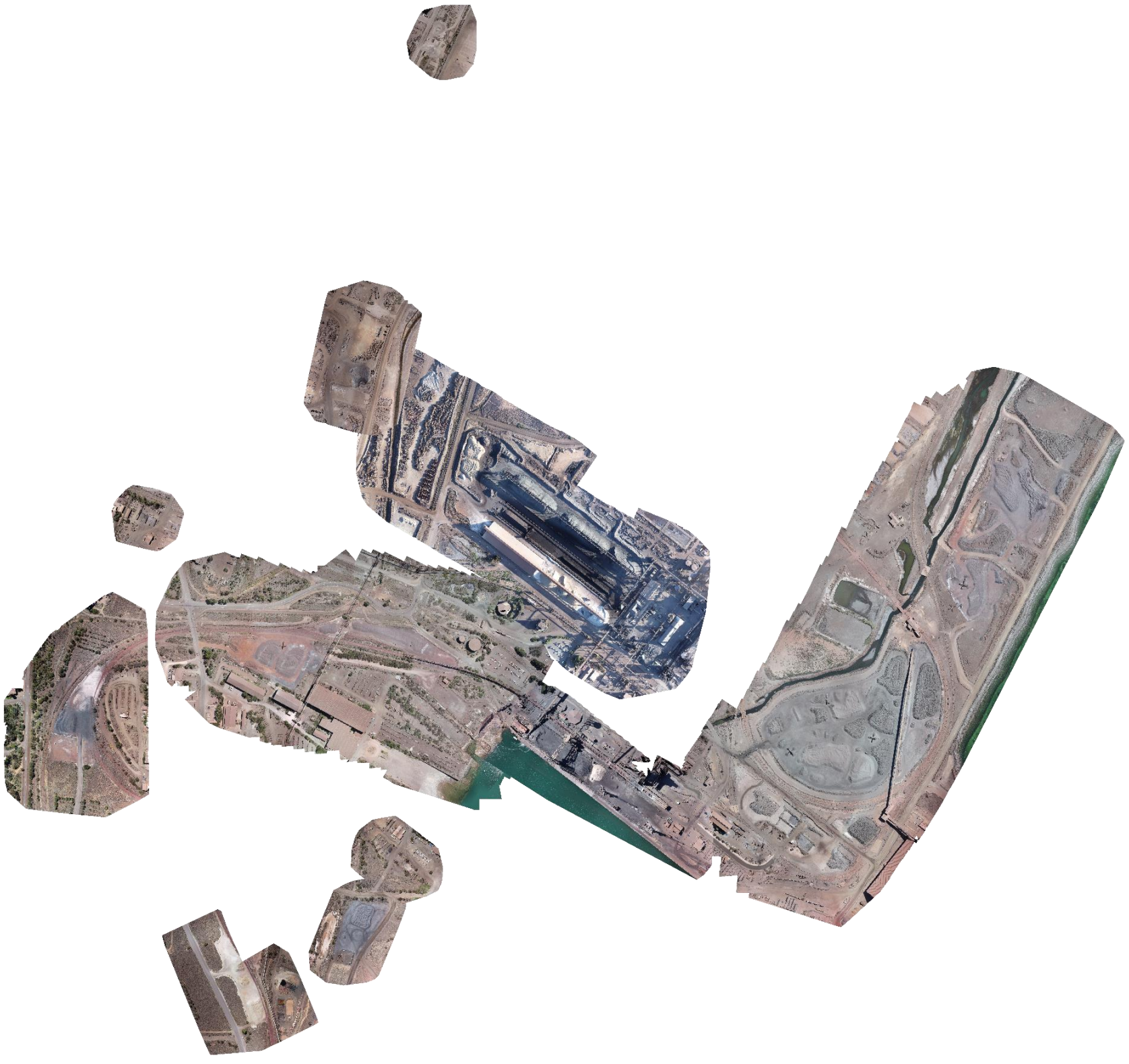

Figure 31: Combined Orthophoto of all sites for February 2023

Figure 32: Combined Orthophoto of all sites for March 2023

Figure 33: Combined Orthophoto of all sites for April 2023

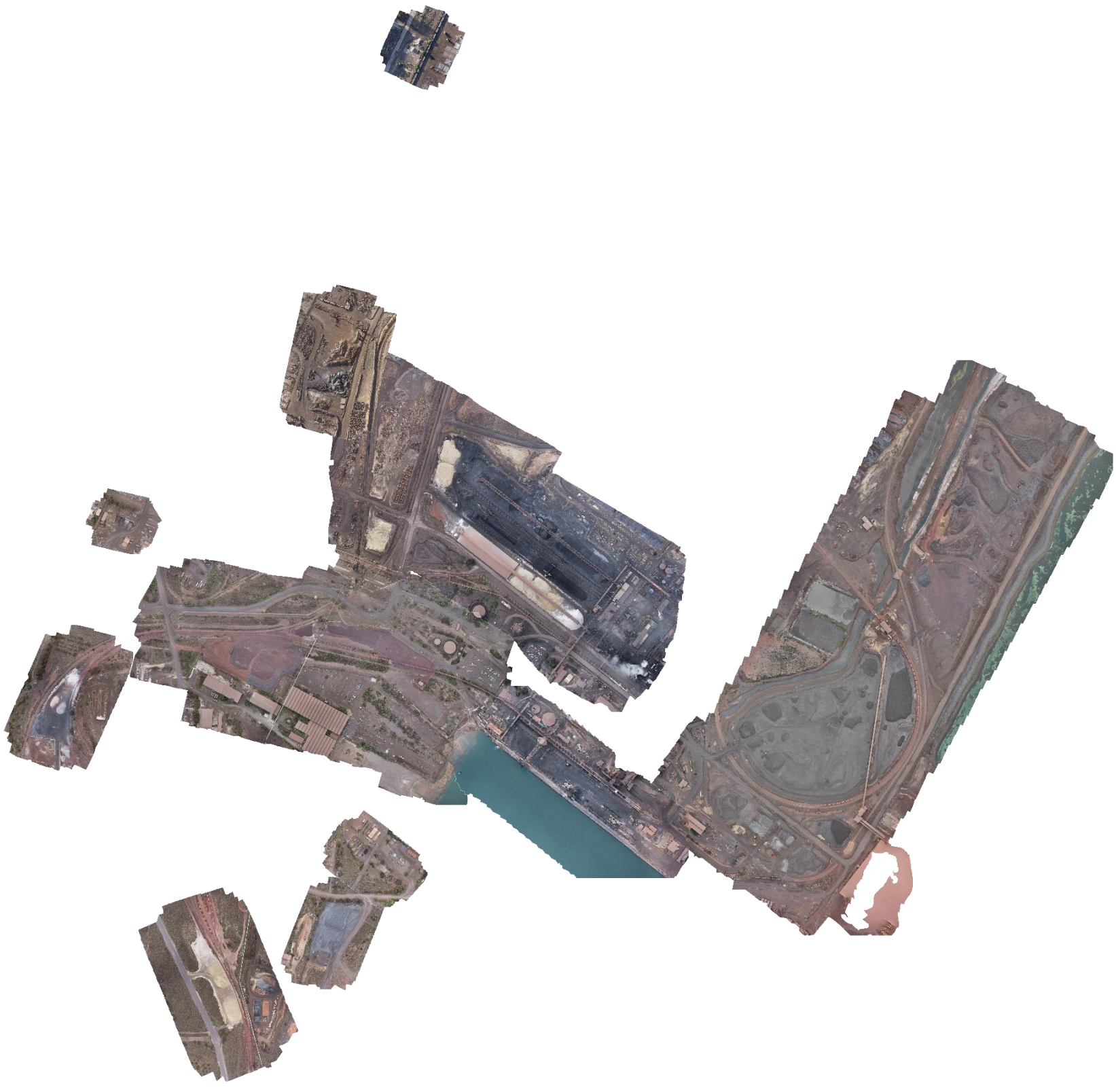

Figure 34: Combined Orthophoto of all sites for May 2023

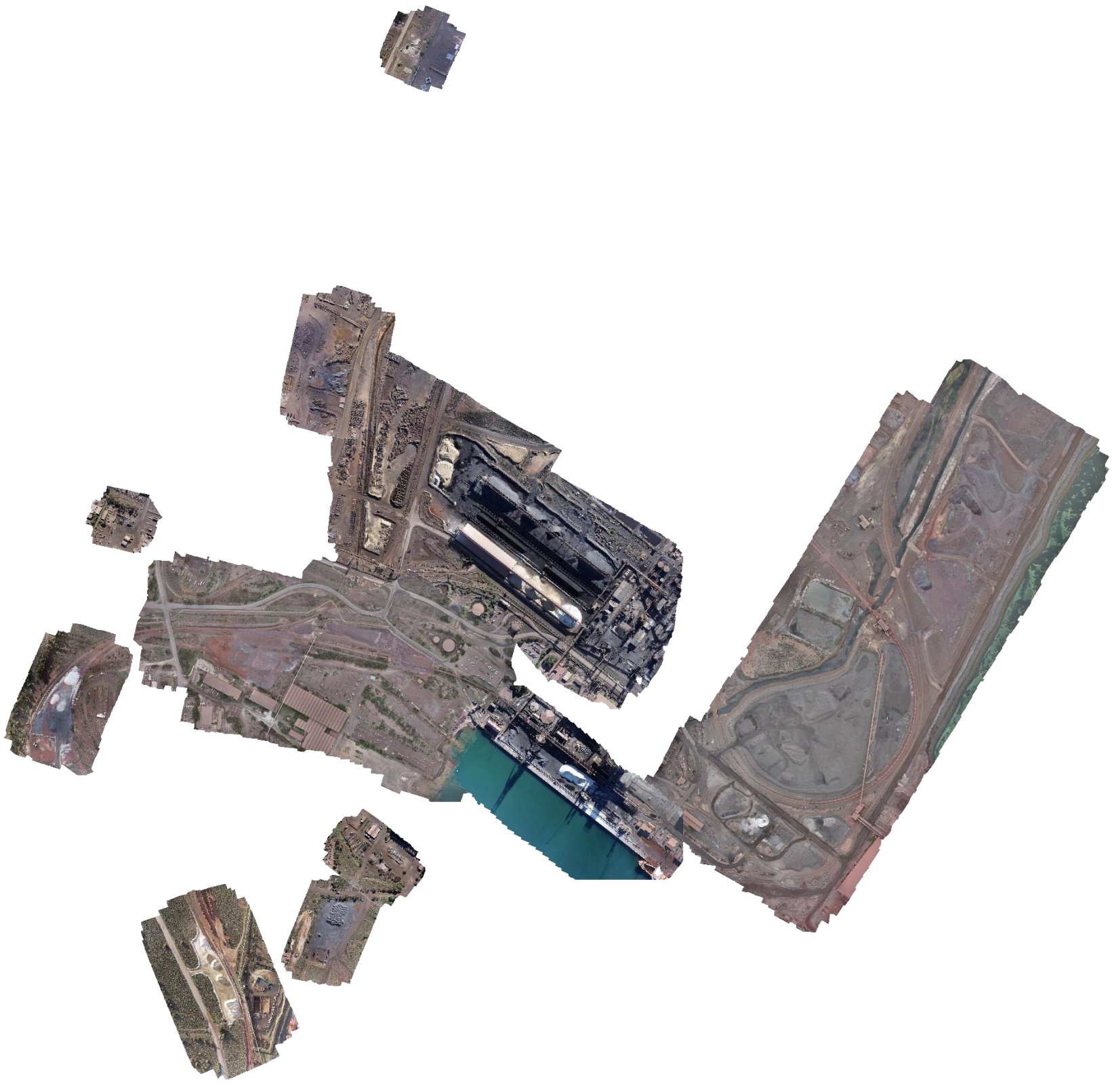

Figure 35: Combined Orthophoto of all sites for June 2023

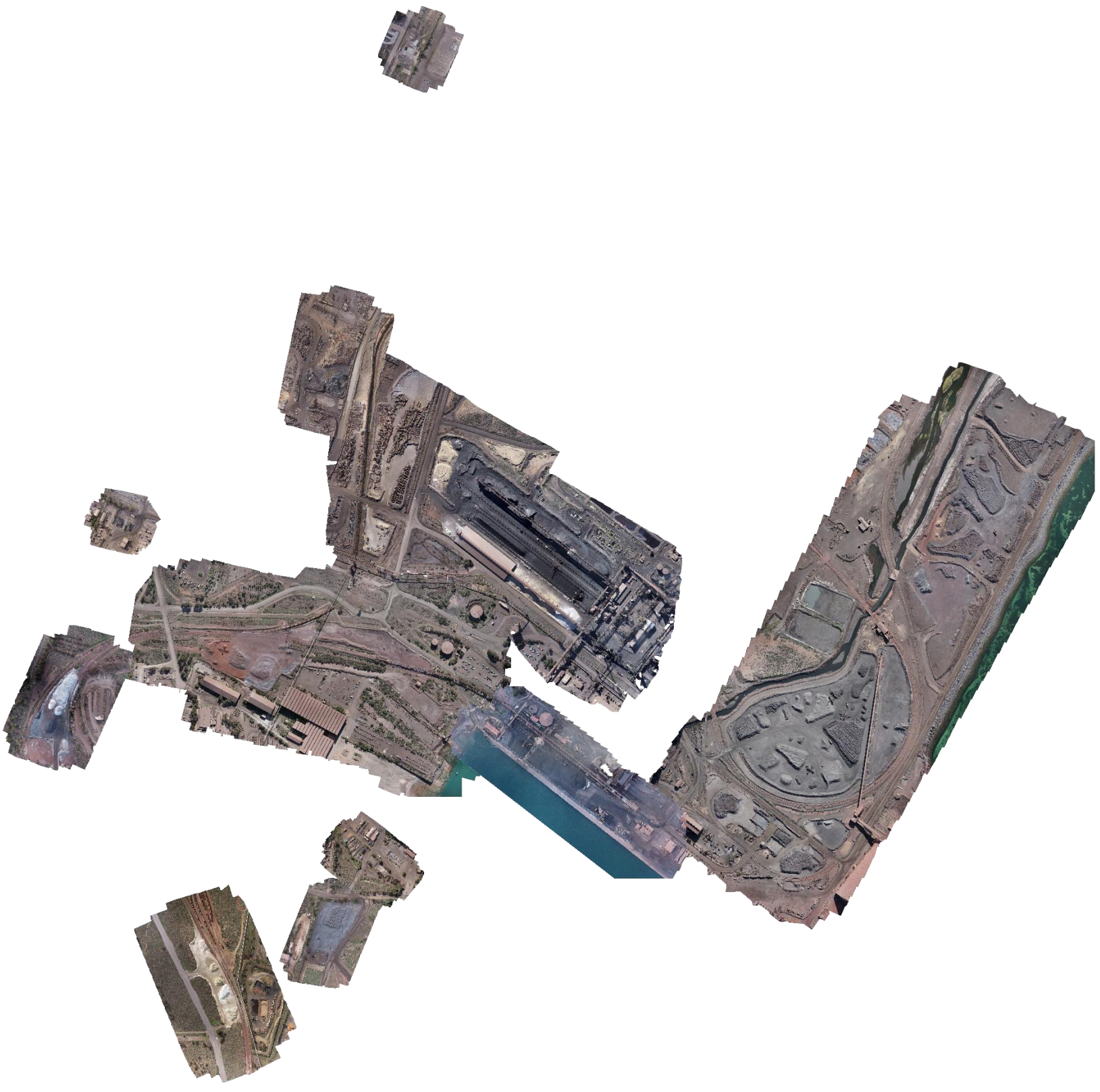

Figure 36: Combined Orthophoto of all sites for July 2023

Figure 37: Combined Orthophoto of all sites for August 2023

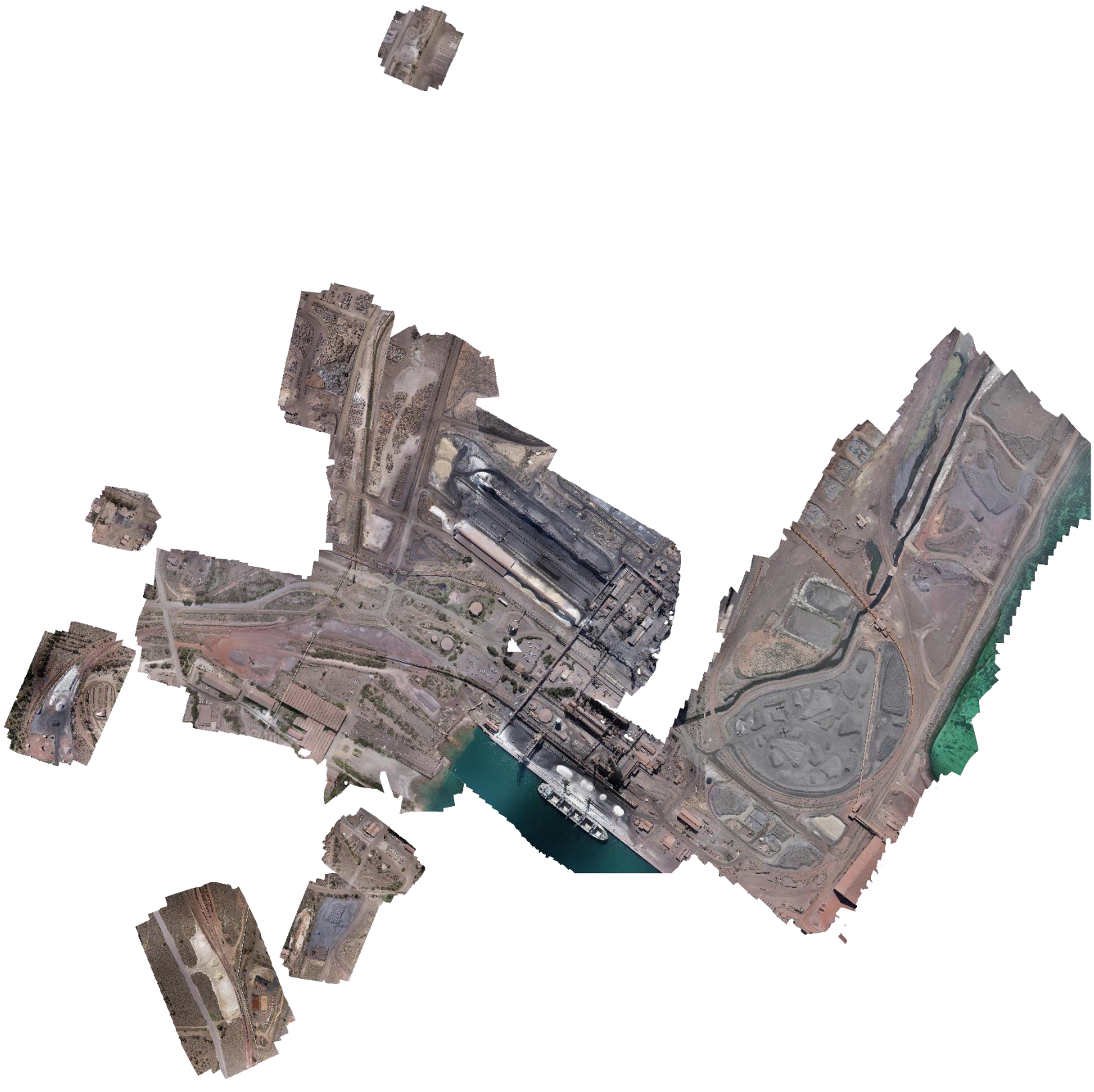

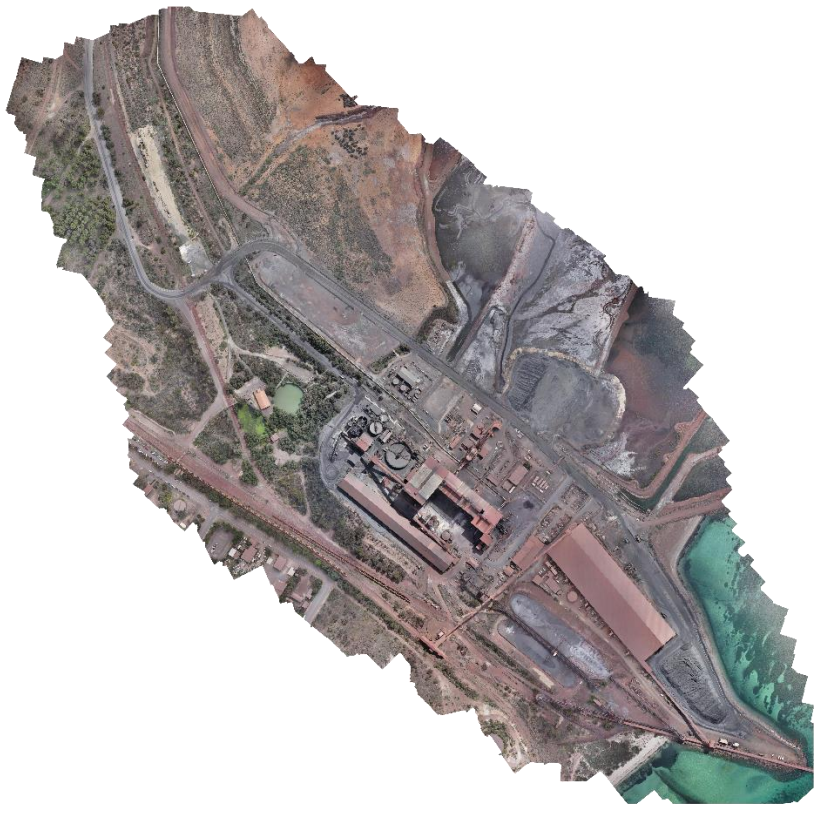

Figure 38: Combined Orthophoto of all sites for September 2023

Figure 39: Combined Orthophoto of all sites for October 2023

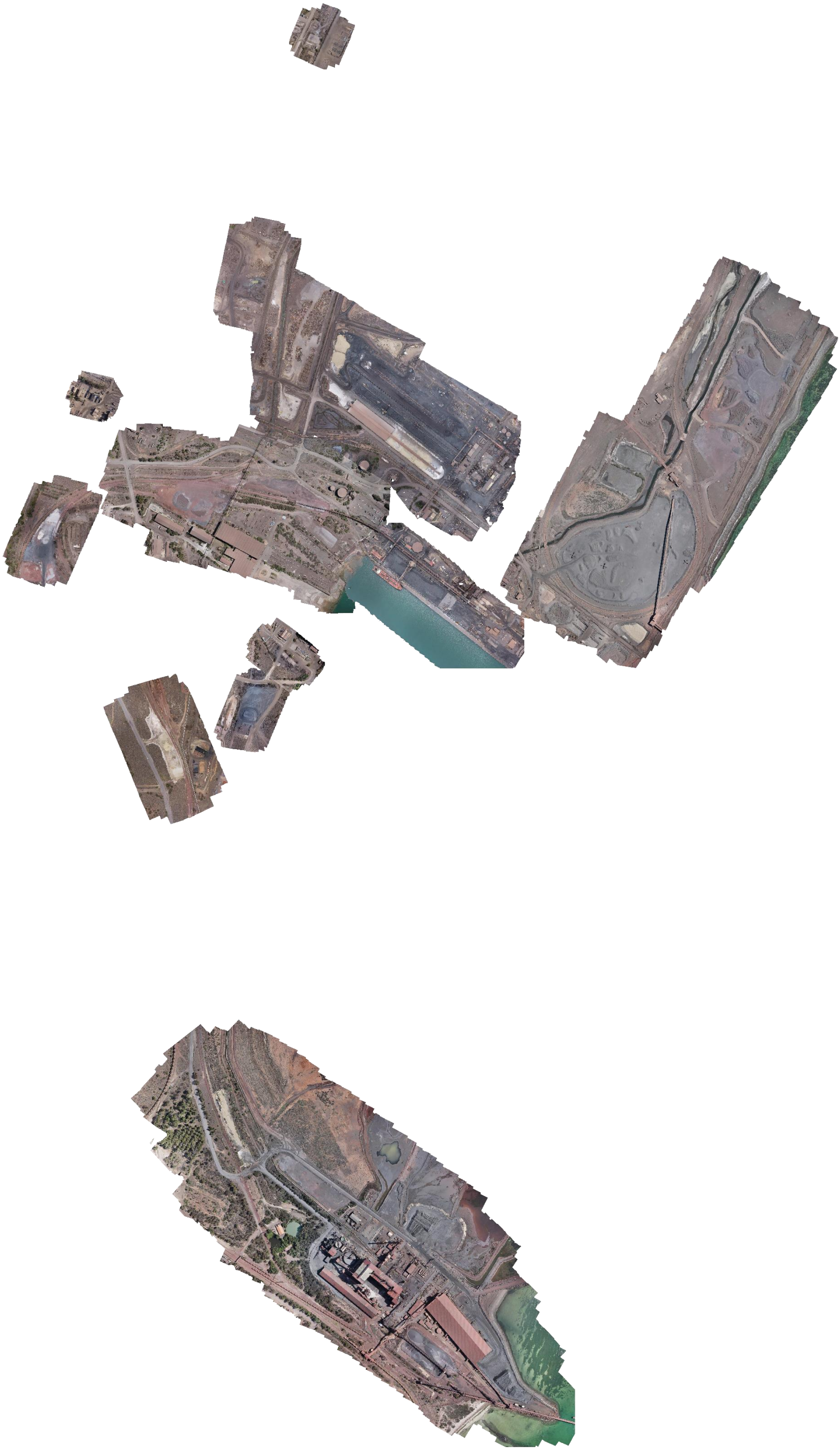

Figure 40: Combined Orthophoto of all sites for November 2023

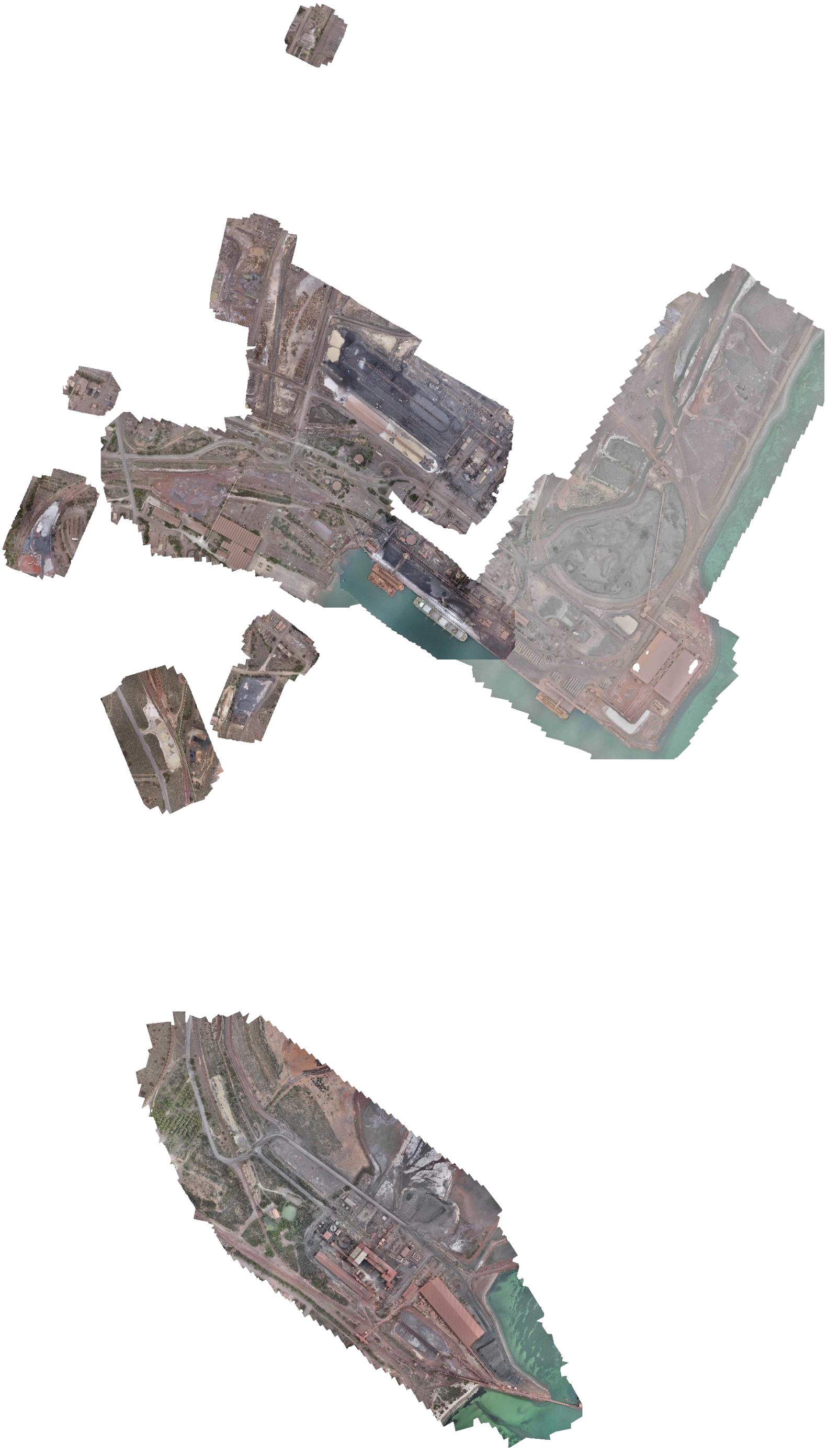

Figure 41: Combined Orthophoto of all sites for December 2023